REVIEW

Check for updates

Hydrogel-based wearable and implantable biosensors in health monitoring

Yutong Wang, Yihan Gao,† Lingfeng Tang,† Yuanyuan Guo, Baoning Sha and Yuanwen Jiang ID *

Hydrogel-based wearable and implantable biosensors have quickly established themselves as a paradigm-shifting platform for continuous health monitoring. They effectively reconcile the mechanical and chemical discrepancies between conventional rigid electronics and delicate biological tissues. This success is largely attributed to the hydrogel material's inherent advantages: high water content, a precisely tunable elastic modulus, and versatile functional chemistry. Collectively, these features provide structural, biological, and processing benefits that facilitate truly seamless bioelectronic integration. This Review systematically summarizes the latest advancements in hydrogel biosensors, placing emphasis on their distinctive material attributes. These include the synergistic ionic–electronic conduction, sensitive stimuli responsiveness, advanced antifouling surface chemistry, and exceptional tissue-mimicking compliance. We further delve into the fundamental physical and chemical sensing mechanisms, supported by representative applications spanning from the non-invasive, real-time analysis of sweat, tears, saliva, and interstitial fluids to the more complex domains of subcutaneous, cardiac, and neural implants. Finally, we candidly address the crucial hurdles that remain, such as long-term hydration stability, signal fidelity drift, and adverse immune responses. Concurrently, we highlight pioneering strategies to overcome these issues, including the adoption of zwitterionic designs for enhanced biocompatibility, nanocomposite reinforcement for mechanical robustness, and the utilization of transient biodegradability. By critically elucidating the intricate relationships governing hydrogel structure, chemistry, and bioelectronic function, this Review aims to chart the research trajectory toward the next generation of durable, self-healing, and fully biointegrated sensing systems.

1. Introduction

The convergence of a globally aging populace and the escalating burden of chronic diseases has generated an acute, unmet clinical demand for technologies capable of continuous, accurate, and non-invasive personal health monitoring. Although conventional clinical diagnostics provide gold-standard precision, their inherent limitations like being centralized, cost-prohibitive, and operationally complex render them fundamentally inadequate for the immediate, personalized requirements of modern preventative medicine. In response, increasing attention has been directed toward system-level and intelligent health monitoring frameworks that integrate continuous physiological data acquisition with real-time analysis and diagnostic decision support, highlighting the importance of persistent, high-quality data streams in disease management and early detection.[1,2] Consequently, wearable and implantable biosensors, which function as the critical translation interface between biological systems and electronics, are rapidly emerging as the cornerstone of a paradigm shift in decentralized health surveillance.

A central bottleneck, however, persists in achieving long-term, high-fidelity bioelectronic integration: the profound mechanical, chemical, and structural mismatch between traditional rigid, inorganic electronic components and the native soft, dynamic, ion-rich biological microenvironment. This severe biotic-abiotic disparity is the primary source of unstable signal transduction, premature mechanical failure, and the induction of a sustained foreign body response, which collectively critically undermine the *in vivo* performance and longevity of sensing platforms.

Hydrogels, a unique and versatile class of polymeric materials, present a highly compelling solution to this "soft–hard" interface conundrum. As three-dimensional (3D) hydrophilic polymer networks capable of absorbing and retaining substantial volumes of water, hydrogels inherently possess a suite of tissue-mimicking characteristics, including ultra-high-

Department of Materials Science and Engineering, the University of Pennsylvania, Philadelphia, Pennsylvania, PA19104, USA. E-mail: ywjiang@seas.upenn.edu
†These authors contributed equally to this work.

water content, a dynamically tunable mechanical modulus, and biologically relevant physicochemical properties. They are thus perfectly positioned to function not only as an ideal conformal bioelectronic interface but also as an active functional matrix for housing sensing elements and facilitating stimuli-responsive behavior.

The landscape of hydrogel-based biosensors and biointegrated electronics has been extensively documented in recent years, with numerous reviews tracking the field's rapid maturation.[3–5] Parallel to these summaries, several landmark studies have introduced sophisticated bioelectronic interfaces characterized by optimized ionic transport and tissue-mimetic mechanics, expanding the possibilities for human–machine interaction.[6–8] Previous reviews have discussed topics such as conductive hydrogels, hydrogel material design, conductive hydrogel networks, flexible bioelectronics, and hydrogel-based sensing platforms for physiological monitoring.[5,9,10] While existing literature offers deep dives into hydrogel synthesis, conductive network design, and general physiological monitoring,[3,5,11] these discussions often remain compartmentalized. A significant gap persists: many current reviews tend to focus exclusively on either the underlying polymer chemistry or specific device architectures, without a systematic framework that links the intrinsic material merits of hydrogels to their specific functional roles in both wearable and implantable contexts.

In this review, we move beyond a general survey to provide a critical and integrated evaluation of recent milestones in hydrogel-enabled biosensing. Our discussion begins by deconstructing the core attributes that render hydrogels ideal sensing matrices, focusing on their structural/chemical synergies and biomimetic properties. We then transition to a rigorous examination of the prevailing physical and chemical transduction mechanisms, scrutinizing their operational limits and the innovative strategies employed to bolster performance. Finally, we showcase the state-of-the-art applications across the sensing continuum, from the non-invasive profiling of biofluids (e.g., sweat, tears, saliva, and interstitial fluid) to high-fidelity implantable interfaces for subcutaneous, cardiac, and neural monitoring. We anticipate that this synthesis will provide the necessary strategic perspectives to steer the development of next-generation biointegrated sensing technologies (Scheme 1).

2. Advantages of hydrogels for wearable and implantable biosensors

Hydrogels are meticulously engineered three-dimensional (3D) polymer networks defined by their capacity to imbibe and stably retain significant volumes of water or biological media without undergoing dissolution. This inherent hydration is driven by the presence of hydrophilic functional groups along the polymer backbone, while the requisite structural integrity is precisely dictated by either covalent or physical crosslinking throughout the matrix. This synergistic structural-chemical

architecture bestows hydrogels with a "soft-solid" rheological character that fundamentally and functionally mimics native biological tissues.[12] Consequently, these materials possess intrinsic and profound advantages as bioelectronic components, specifically by providing a physiologically relevant hydrated microenvironment, facilitating superior mechanical compliance, and serving as an easily tunable matrix for diverse functional modifications.

Building upon these fundamental material characteristics, hydrogels exhibit distinct and unique advantages when integrated into wearable and implantable biosensing technologies. For clarity, these merits are systematically categorized in the following sections into structural/chemical attributes and biological/biomimetic properties, which collectively demonstrate why hydrogels are uniquely positioned as the leading candidate material for next-generation bio-integrated sensing platforms.

2.1. Structural and chemical advantages

2.1.1. 3D porous architecture. The Three-dimensional (3D) porous architecture is a defining characteristic of hydrogels that is instrumental to their performance in wearable and implantable biosensors.[13] This structural feature directly contributes to enhanced sensitivity and rapid response kinetics by maximizing the functional interface area and accelerating mass transport in complex physiological settings.[14] Specifically, the interconnected network amplifies binding events, sustains analyte flux, mitigates fouling, and stabilizes transduction over periods of continuous monitoring, allowing porous hydrogels to consistently outperform dense polymer matrices.

The optimized structure inherently reduces diffusion resistance and significantly increases the active-site density.[15] Furthermore, channels engineered with tuned tortuosity facilitate the swift delivery of critical analytes, such as glucose, lactate, and inflammatory biomarkers, to the sensing interface, thereby minimizing the overall response time.[14] The expanded interfacial area also enables highly efficient anchoring of recognition elements, including enzymes, aptamers, and antibodies, which, in turn, dramatically boosts the signal-conversion sensitivity.[15] In electrochemical formats, the open network promotes cooperative ionic and electronic conduction paths, which simultaneously enhances interfacial current while attenuating background noise.[16] Collectively, the combined benefits of accelerated mass transport, heightened interfacial activity, and streamlined charge conduction act synergistically to elevate overall biosensor performance.

Illustratively, Kim et al.[17] fabricated a nanofiber hydrogel patch featuring high porosity via electrospinning; the resulting porous network significantly accelerated glucose diffusion, achieving both a rapid response time (<15 s) and a remarkably low detection limit (0.01 mM). Similarly, Singh et al.[18] demonstrated the utility of a macro-porous poly (ethylene glycol) (PEG) cryo-gel for one-step aptamer selection. In this case, the optimized pore size enabled the passive diffusion of low-affinity oligonucleotides away from the matrix while selectively
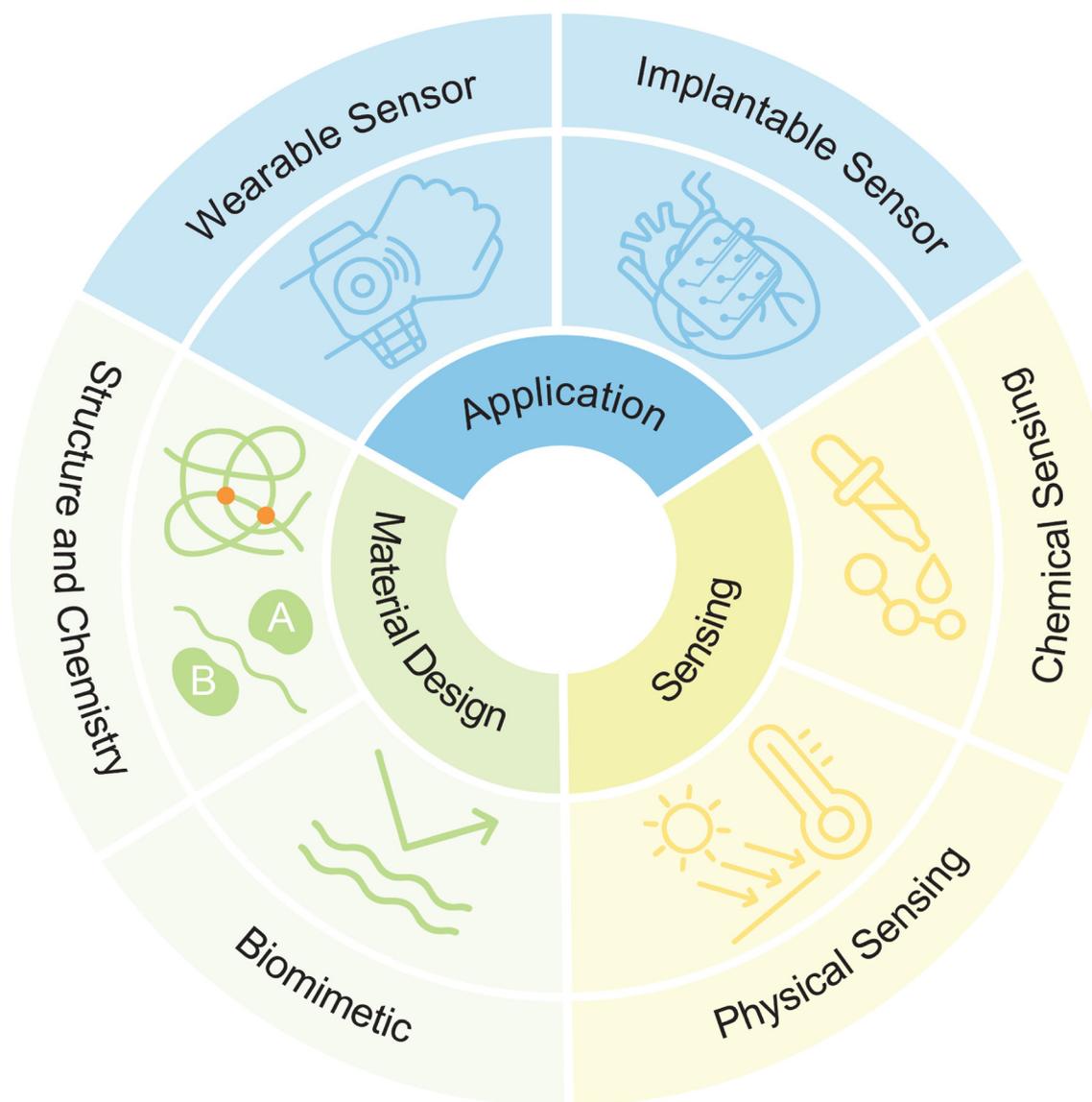
Scheme 1 Hydrogel-based wearable and implantable biosensors overview.

retaining high-affinity sequences, thereby substantially improving enrichment efficiency and binding stability.

In conclusion, the 3D porous architecture is critical for augmenting both mass transport kinetics and interfacial activity, thus enabling hydrogel-based biosensors to achieve superior sensitivity and response speed. Beyond these structural benefits, hydrogels also offer a wealth of functional groups for chemical modification, which play an equally pivotal role in device functionalization and performance enhancement.

2.1.2. Functional groups availability. Hydrogels possess a wide array of accessible functional groups that are foundational to their exceptional chemical tunability.[13] Specifically, moieties such as carboxyl, hydroxyl, amino, and thiol groups provide precise chemical handles, enabling researchers to graft diverse recognition elements, securely immobilize essential biomolecules, and strategically engineer signal transduc-

tion pathways.[19,20] Relative to chemically inert matrices, these highly reactive functional groups drastically expand the design space and enhance the programmability of both wearable and implantable biosensing formats.[13]

Mechanistically, these chemical groups serve dual roles as both molecular anchors and signal mediators.[21] Carboxyl and amino groups, for instance, are commonly utilized to form stable covalent bonds with enzymes, antibodies, or aptamers, a process essential for preserving their long-term bioactivity during continuous sensing.[21] This same facile chemistry is leveraged to program molecular selectivity[19] and to dynamically enhance swelling characteristics and ionic conductivity, thereby creating a highly hydrated microenvironment that expedites analyte diffusion and significantly amplifies signal transduction. Furthermore, the introduction of dynamic and reversible linkages, such as those based on Schiff-base or boro-

nate ester chemistries can impart desirable features like self-healing capacity and tunable binding affinity, which collectively boost mechanical resilience and stabilize device performance in demanding *in vivo* and wearable applications.[22]

These principles are convincingly validated in recently reported sensor designs. Elsherif *et al.*,[23] for example, engineered a phenylboronic-acid (PBA)-functionalized hydrogel film for glucose detection. In this system, the PBA moiety reversibly binds the *cis*-diol groups of glucose, triggering a controlled and quantifiable volumetric change within the hydrogel network. By strategically integrating micro-patterned structures to amplify the resultant optical shifts, their platform achieved ultra-sensitive glucose monitoring with an exceptionally low detection limit. Similarly, Shen *et al.*[24] developed a photonic hydrogel sensor by covalently linking amino-terminated aptamers to a carboxyl-rich matrix *via* amide coupling. Upon binding to thrombin, the aptamers modulated the effective crosslinking density, which resulted in an alteration of the photonic crystal structure's diffraction, enabling nanomolar-level detection with remarkable stability in human serum.

Beyond simple molecular functionalization, the spatial engineering of hydrogel networks has also been explored as a means to regulate analyte transport and enrichment. A representative example is the work by Han *et al.*,[25] who developed a gradient P(AA–AM–NH$_2$–β-CD) hydrogel through unilateral UV-induced polymerization. In this design, a controlled gradient in polymer chain density creates an internal potential that drives the autonomous enrichment of target species. Such spatially graded architectures offer a practical strategy for enhancing mass transport and analyte preconcentration, capabilities that directly benefit the sensitivity and overall performance of hydrogel-based sensing interfaces.

In summary, the availability of these diverse chemical functionalities permits precise molecular engineering and stable biomolecular immobilization within the hydrogel matrix, effectively translating specific molecular recognition events into robust and quantifiable electrical or optical signals. This level of chemical programmability is ultimately paramount for elevating the sensitivity, selectivity, and long-term durability of next-generation hydrogel biosensors.

2.1.3. Electrical and ionic conduction. Exceptional electrical and ionic conduction imbues hydrogels with a distinct and critical advantage for both wearable and implantable biosensing applications. Unlike conventional insulating polymeric materials, hydrogels inherently provide hydrated ionic channels and can be readily engineered through the incorporation of conductive polymers or nanomaterials to facilitate electronic transport. This coupling enables the rapid and highly efficient interconversion between ionic signals (native to the body) and electronic signals (required by the device) within a unified platform.[26] Consequently, hydrogels intrinsically interface seamlessly with physiological electrochemical processes, delivering sensitive and remarkably stable signals during real-time monitoring.

The mechanism of hydrogel conduction relies on the synergistic interplay between the hydrated polymer network and the added conductive components. The water-rich structure and hydrophilic functional groups establish continuous ionic pathways that permit the rapid migration of Na$^+$, K$^+$, and Cl$^-$ ions, which fundamentally minimizes mass-transfer resistance and significantly accelerates sensor response kinetics.[27] Complementarily, the judicious incorporation of conductive polymers (*e.g.*, PEDOT:PSS, polyaniline), carbon nanomaterials (*e.g.*, CNTs, graphene), or 2D materials (*e.g.*, MXene) establishes robust electronic conduction networks that complement the ionic migration.[28] This dual-channel transport mechanism dramatically enhances interfacial charge transfer and signal amplification, thereby directly leading to improved detection sensitivity for low-concentration analytes. Moreover, the effective coupling of ionic and electronic conduction acts to attenuate noise and stabilize signal fidelity, which is paramount for enabling long-term, real-time monitoring in chronic wearable and implantable devices.[29]

The efficacy of this ion–electron cooperation is powerfully demonstrated in recent advanced hydrogel designs. Rong *et al.*[30] constructed a three-dimensional poly-pyrrole (PPy)/gold-nanoparticle hydrogel, which successfully combined high electronic conductivity (0.46 S cm^{-1}) with an ultra-high water content 94.5 wt%. The material provided simultaneous, high-efficiency electronic and ionic channels, allowing a carcinoembryonic-antigen (CEA) immunosensor to achieve an ultralow detection limit of 0.16 fg mL^{-1} across an exceptionally wide linear range 1 fg mL^{-1}–200 ng mL^{-1}. This outcome serves as a compelling testament to how ion–electron synergy amplifies charge transfer and sensitivity. In a related approach, Xue *et al.*[31] pioneered a bilayer conductive hydrogel electrode for long-term electroencephalography (EEG) monitoring. They utilized PEDOT:PSS for electronic transport and incorporated KCl to ensure robust ionic mobility within the hydrated network. This optimized dual-channel configuration reduced the skin–electrode impedance to below 0.4 kΩ, significantly lower than the ~15 kΩ typical of dry electrodes, and critically maintained this stability for 12 hours, a marked improvement over the mere 4 hour lifespan of standard wet electrodes.

In conclusion, these studies unequivocally establish that hydrogels achieve superior performance through the effective integration of ionic and electronic pathways. This enhanced charge transport, coupled with improved sensitivity and stability, also enables adaptation to various environmental stimuli (*e.g.*, pH, temperature, glucose concentration), positioning these materials as key enablers for next-generation, self-regulating biosensors.

2.1.4. Stimuli-responsiveness. Stimuli responsiveness is a defining feature that decisively distinguishes hydrogels as exceptionally powerful materials for both wearable and implantable biosensors. Their soft, three-dimensional polymer networks harbor dynamic and chemically sensitive motifs that undergo reversible reorganization, swelling, or contraction in response to environmental fluctuations, such as changes in pH, temperature, glucose concentration, ionic strength, or reactive oxygen species.[32] These dynamic, reversible transformations directly translate external environmental cues into quantifiable electrical

or mechanical outputs, thereby allowing hydrogels to orchestrate high-precision, real-time physiological monitoring.

2.1.4.1. Mechanical stimuli. Mechanical stimuli can be leveraged to induce deformation within the hydrogel matrix, triggering corresponding functional responses. Wei *et al.*,[33] for example, engineered an artificial-cilia array capable of decoding acoustic frequencies to orchestrate resonance-guided drug release. Utilizing 3D printing, they fabricated cilia with diameters between 40–200 μm and high aspect ratios of 30–100. When these cilia vibrated under incident sound waves, they imparted dynamic mechanical forces onto the underlying hydrogel, which in turn triggered the controlled release of insulin and glucagon in a Type 1 diabetes model.

2.1.4.2. Thermal inputs. Thermal inputs similarly provide a powerful means to govern hydrogel conformation. Mok *et al.*[34] pioneered thermoresponsive micro-hydrogel sensors (μTAMs) to map tissue mechanics in 3D. These sensors utilized poly(*N*-isopropylacrylamide) (PNiPAAm), a material that undergoes volumetric expansion below its lower critical solution temperature (~34 °C). Crucially, the magnitude of the swelling response accurately reflected the local matrix elasticity, enabling the team to chart micrometer-scale stiffness landscapes. Using this methodology, they successfully identified stiffness "hotspots" exceeding 250 kPa within invasive breast-cancer spheroids, thereby exposing mechanical heterogeneity directly linked to tumor invasion (Fig. 1C).

2.1.4.3. Magnetic stimuli. Magnetic stimuli offer a unique avenue for amplifying molecular recognition through the reconfiguration of integrated nanoparticles. Chen *et al.*[35] devised the MATCH platform (Magnetic Augmentation through Triple-Gradient Coupling), which innovatively integrated DNA-responsive hydrogels with a spatially patterned magnetic-nanoparticle gradient. Upon binding the target biomarker, the hydrogel network reorganized, modulating the magnetic alignment and producing measurable signal shifts. The MATCH platform successfully detected as few as ~10 RNA copies and ~1000 protein copies in plasma within 60 minutes, critically bypassing the need for labeling and washing steps (Fig. 1B).

2.1.4.4. Immuno-responsive architectures. Immuno-responsive hydrogels represent a specialized class that directly translates antigen–antibody recognition into quantifiable electrical signatures. Li *et al.*[36] successfully coupled antibody-functionalized hydrogels to radio frequency resonators. Antigen binding specifically disrupted crosslinks, inducing measurable hydrogel swelling, which consequently shifted the resonant frequency. This sophisticated method achieved an ultrasensitive detection limit in the femtogram-per-liter range (Fig. 1A).

2.1.5 Antifouling chemistry. Antifouling chemistry constitutes another pivotal advantage distinguishing hydrogels for use in wearable and implantable biosensors. Unlike materials based on conventional polymers, hydrogel surfaces can be
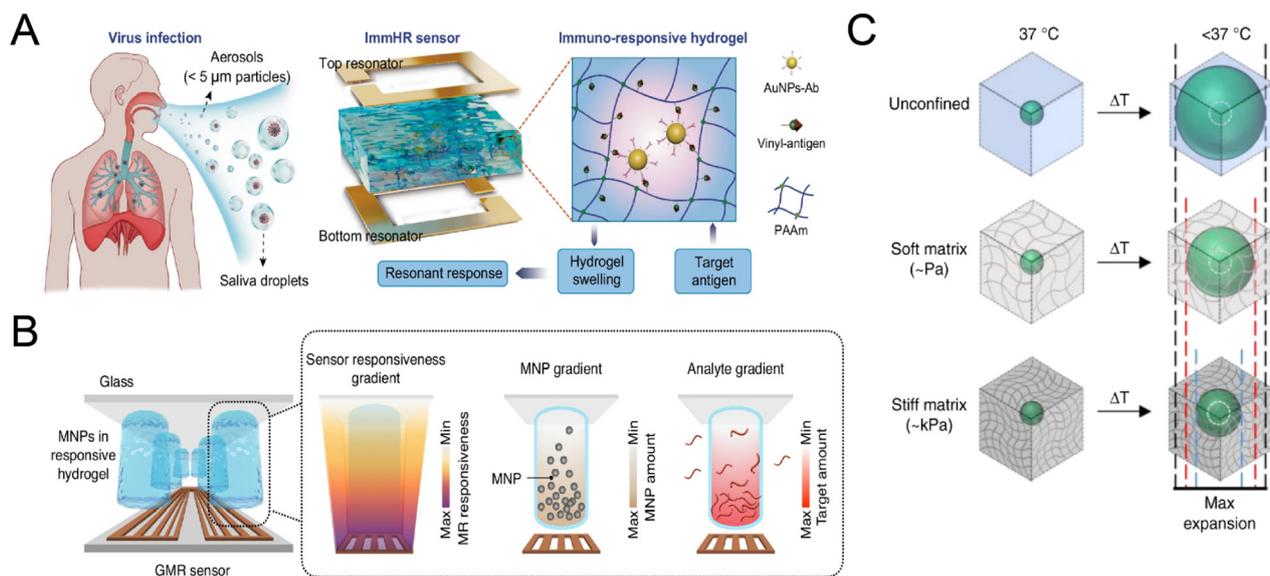

Fig. 1 Demonstrative examples of stimuli-responsive hydrogel biosensors. (A) Immuno-responsive hydrogel resonator sensor for antigen–antibody recognition. Target binding induces hydrogel swelling, leading to a shift in the resonant frequency, enabling highly sensitive detection. Reproduced from ref. 36 with permission from [Springer Nature], [Xin Li *et al.*, *Nature Communications*, 2024] https://doi.org/10.1038/s41467-024-48294-1, under a Creative Commons CC BY 4.0 license, copyright 2024. (B) Magnetically responsive hydrogel sensor (MATCH platform) incorporating spatially patterned magnetic-nanoparticle gradients for amplified molecular recognition of low-concentration biomarkers. Reproduced from ref. 35 with permission from [Springer Nature], [Yuan Chen *et al.*, *Nature Communications*, 2024] https://doi.org/10.1038/s41467-024-52754-z, under a Creative Commons CC BY 4.0 license, copyright 2024. (C) Thermo-responsive micro-hydrogel sensors (μTAMs) that exhibit expansion below the lower critical solution temperature (~34 °C). The magnitude of swelling accurately reflects local matrix stiffness, enabling high-resolution 3D mechanical mapping of biological tissues. Reproduced from ref. 34 with permission from [Springer Nature], [Stephanie Mok *et al.*, *Nature Communications*, 2020] https://doi.org/10.1038/s41467-020-18469-7, under a Creative Commons CC BY 4.0 license, copyright 2020.

designed to maintain a dense, organized hydration layer and can be further functionalized with poly (ethylene glycol) (PEG)-based or zwitterionic moieties that actively suppress the non-specific adsorption of proteins, cells, and microbial contaminants.[37]

The underlying mechanisms of this robust antifouling performance are multifaceted, relying on a combination of physically tailored hydration, precise chemical modification, and dynamic surface functionality. The dense interfacial water layer forms an effective physical barrier that sterically repels biomacromolecule adsorption. Complementarily, zwitterionic or PEG-based groups are incorporated to enhance surface energy homogeneity and near-zero electrostatic neutrality, thereby minimizing adhesion events.[38] Furthermore, the incorporation of dynamic chemical functionalities, such as those based on reversible hydrogen bonding or ionic coordination, maintains surface flexibility and mobility, which further acts to kinetically destabilize nonspecific interactions.[39] Collectively, these sophisticated antifouling strategies are essential for minimizing signal drift and background noise, enabling hydrogels to maintain clean interfaces and deliver stable, highly sensitive performance during long-term monitoring in complex physiological environments.[40]

The critical impact of advanced antifouling design has been convincingly demonstrated across diverse hydrogel systems. Sabaté del Río *et al.*[41] engineered an affinity-based electrochemical biosensor using a three-dimensional cross-linked bovine serum albumin (BSA) coating integrated with gold nanowires, nanoparticles, and carbon nanotubes. This hybrid coating successfully resisted nonspecific adsorption in complex biofluids and critically retained approximately ~88% of its initial signal after one month of continuous operation in unprocessed human plasma. Moreover, the sensor quantified IL-6 with high accuracy, underscoring how antifouling chemistry effectively stabilizes electron transfer kinetics and significantly extends sensing lifetime. In another demonstration, Wang *et al.*[42] developed a semi-dry conductive hydrogel electrode for electroencephalography (EEG) monitoring with intrinsic antibacterial properties. Constructed from poly (*N*-acryloyl glycinamide) (PNAGA) and a chitosan derivative, the electrode effectively inhibited the colonization of *E. coli* and *S. epidermidis*. In human trials, the electrode maintained stable performance over 12 hours of continuous wear, exhibiting an average contact impedance of <400 Ω and a signal-to-noise ratio SNR ≈20.02 dB. This compellingly demonstrates that incorporating antibacterial chemistry directly mitigates biofouling at the skin–electrode interface, thereby preventing the progressive increase in impedance and accumulation of noise, which is essential for ensuring stable, long-term signal acquisition. Furthermore, Tohamy[43] introduced a fluorescent antimicrobial hydrogel (CM-Hemi@Ca-N-CDs) derived from carboxymethyl hemicellulose and nitrogen-doped carbon dots. Beyond its use in microbial sensing, the hydrogel exhibited potent antimicrobial activity, yielding inhibition zones of ~13 mm against *E. coli*, and ~15 mm against *S. aureus*. The hydrogel's ability to block microbial colonization and hinder biofilm formation at the sensor interface is vital for reducing background interference and prolonging the overall longevity of the device.

2.2. Biological and biomimetic advantages

2.2.1. Bionic properties.
The advancement of flexible bioelectronic devices has inaugurated new frontiers in health monitoring, disease diagnostics, therapeutics, and human–machine interfacing. Nevertheless, establishing stable, long-term coupling between electronic systems and soft, dynamic biological tissues remains a formidable central challenge. Conventional electrodes, typically fabricated from rigid materials like metals, silicon, or stiff polymers, offer excellent conductivity and mechanical robustness but fundamentally diverge sharply from native biological tissues in terms of elasticity and interfacial chemistry. Human soft tissues (*e.g.*, skin, muscle, nerve, brain) exhibit Young's moduli ranging from hundreds of pascals to tens of kilopascals, whereas traditional inorganic electronic materials span the megapascals to gigapascals range, resulting in a stiffness mismatch of up to six orders of magnitude.[3] This mechanical disparity is the root cause of interfacial delamination, signal instability, and the inevitable induction of chronic inflammation and immune rejection during prolonged implantation.[44] Furthermore, the dry, ion-deficient surfaces of inorganic materials critically impede molecular exchange, thereby limiting effective bioelectronic communication.

Hydrogels decisively overcome these profound limitations through their intrinsically bionic nature. They are composed of hydrophilic polymer chains cross-linked into a porous 3D network that retains substantial amounts of water, authentically recreating the hydrated microenvironment of the extracellular matrix (ECM). Crucially, their mechanical behavior can be precisely tailored through chemical or physical cross-linking, or by engineering advanced composite architectures. This tunability allows moduli to be aligned closely with living tissues, spanning from a few hundred pascals to several hundred kilopascals. Consequently, hydrogels integrate two essential bionic advantages: high water content and mechanical modulus matching. These combined features guarantee superior interfacial stability and robust long-term biocompatibility, establishing hydrogels as an indispensable material cornerstone for next-generation biosensors (Fig. 2A).

2.2.1.1. High water content. High water content is the preeminent feature that distinguishes hydrogels from traditional rigid electronic materials and underpins many of their bioelectronic advantages. Most hydrogels retain 70–95% water, with certain advanced systems exceeding 95%. Such a hydrated, ion-rich environment closely mimics the native ECM, providing optimal conditions for both efficient signal transmission and robust cellular survival.

Electrically, the abundant aqueous phase establishes a low-impedance interface between the tissue and the electrode. Given that impedance is governed by both charge transfer and ionic diffusion, the highwater content of hydrogels furnishes continuous ionic pathways that form a "hydrated conductive
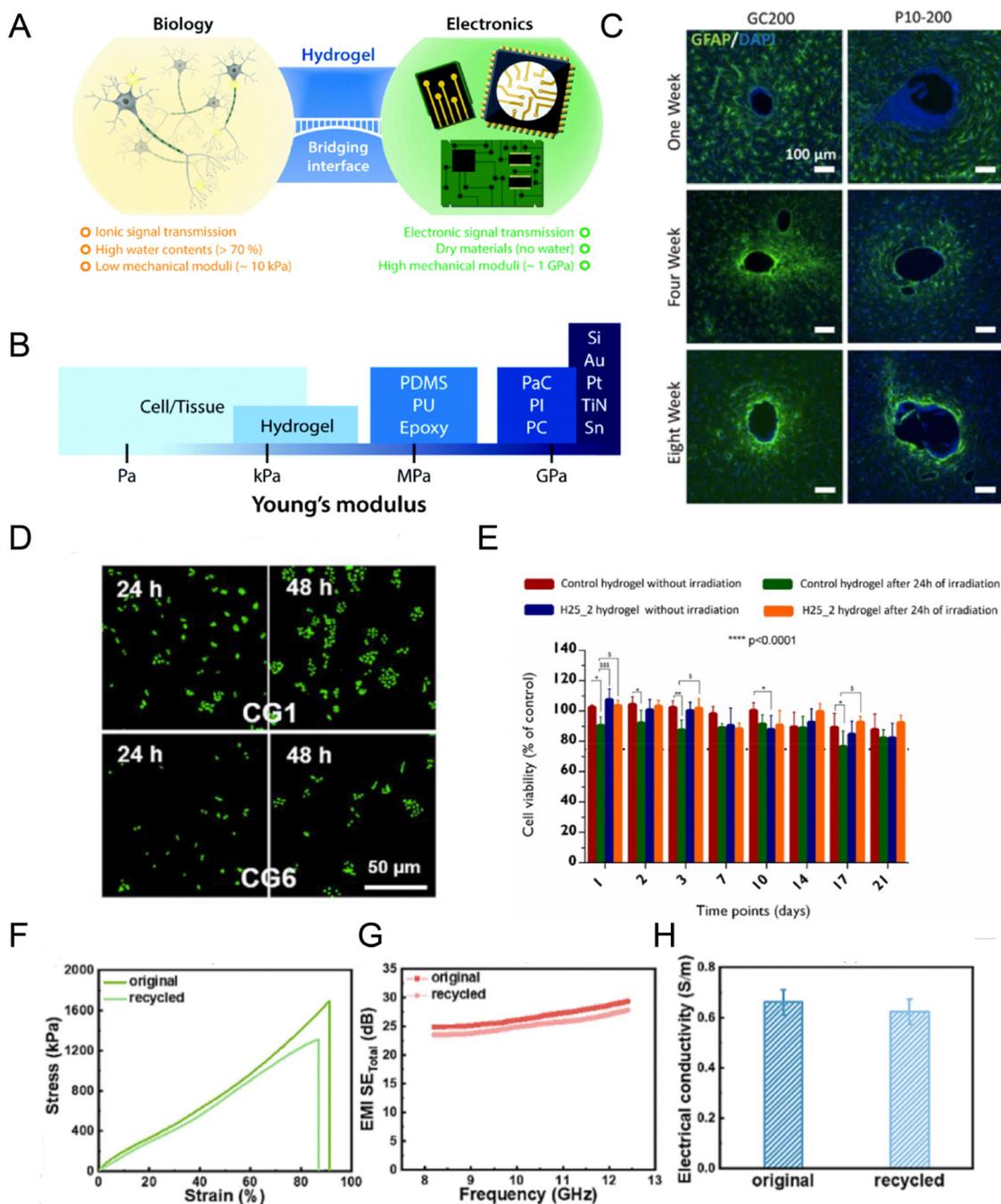
Fig. 2 Biological and biomimetic features of hydrogels. (A) Hydrogels at the interface between biology and electronics. Reproduced from ref. 3 with permission from [Royal Society of Chemistry], [Hyunwoo Yuk *et al.*, *Chemical Society Reviews*, 2019] https://doi.org/10.1039/C8CS00595H, under a Creative Commons CC BY-NC 3.0 license, copyright 2019. (B) Young's moduli of cell/tissue and common electrode materials. Reproduced from ref. 3 with permission from [Royal Society of Chemistry], [Hyunwoo Yuk *et al.*, *Chemical Society Reviews*, 2019] https://doi.org/10.1039/C8CS00595H, under a Creative Commons CC BY-NC 3.0 license, copyright 2019. (C) Reduced glial scarring around hydrogel-coated implants *versus* uncoated glass capillaries at 1, 4, and 8 weeks. Reproduced from ref. 3 with permission from [Royal Society of Chemistry], [Hyunwoo Yuk *et al.*, *Chemical Society Reviews*, 2019] https://doi.org/10.1039/C8CS00595H, under a Creative Commons CC BY-NC 3.0 license, copyright 2019. (D) hydrogel can support HEK-293 cell proliferation. Reproduced from ref. 46 with permission from [Elsevier], [Rui Yin *et al.*, *Journal of Materials Science & Technology*, 2023] https://doi.org/10.1016/j.jmst.2022.10.047, copyright 2023. (E) Results of *in vitro* cell viability when cells are exposed to gel conditioned medium. Reproduced from ref. 47 with permission from [Elsevier], [Rita G. Fonseca *et al.*, *Materials Today Bio*, 2022] https://doi.org/10.1016/j.mtbio.2022.100325, under a Creative Commons CC BY-NC-ND 4.0 license, copyright 2022. Comparisons of the original and recycled RG6 hydrogels in: (F) tensile curves, (G) EMI SE and (H) electrical conductivity. Reproduced from ref. 48 with permission from [Elsevier], [Rui Yin *et al.*, *Chemical Engineering Journal*, 2023] https://doi.org/10.1016/j.cej.2023.145794, copyright 2023.

medium" seamlessly bridging the electrode to the tissue. This architecture fundamentally reduces bulk resistance and eliminates the high contact impedance characteristic of dry electrodes. Yuk et al.[3] demonstrated that water-rich hydrogels adhere intimately to the skin while actively preserving tissue hydration, a dual action that stabilizes signal acquisition in EEG, ECG, and TENS applications. In a related study, a conductive hydrogel with approximately 85% water content was developed.[49] Its ion–electron dual-channel network not only maintained tissue-like softness but also significantly enhanced interfacial electrical performance, enabling effective neural stimulation at an ultralow driving voltage of just 50 mV. This marked reduction in energy consumption is a pronounced advantage over traditional cuff electrodes, which typically require far higher driving voltages.

Biologically, high water content profoundly enhances cellular compatibility. By reproducing the moist microenvironment of native tissues, hydrated hydrogels facilitate crucial nutrient transport and shield cells from dehydration-induced stress. The continuous free water phase enables the efficient diffusion of metabolites, while the structured hydration layers prevent detrimental protein denaturation and cell membrane disruption. Annabi et al.[50] reported that MeTro/GO hybrid hydrogels, containing nearly 90% water, supported robust adhesion and proliferation of cardiomyocytes, confirming that optimized hydration is vital for sustaining long-term cellular functionality.

Beyond inherent biocompatibility, high-water-content structures enable sophisticated multimodal sensing. The continuous aqueous phase contains mobile ions that respond dynamically to mechanical, thermal, and chemical stimuli. When the hydrogel is subjected to stretch or compression, the ionic pathways reconfigure, altering capacitance and conductivity to register strain or pressure. Similarly, thermal fluctuations accelerate ion diffusion and induce network swelling, yielding a decrease in resistance with rising temperature. Concurrently, the hydrated matrix facilitates the rapid diffusion of small molecules, allowing hydrogels to detect shifts in pH, metabolites, or inflammatory biomarkers. Lei et al.[51] leveraged these integrated properties in a "bio-inspired ionic skin" that achieved real-time capacitive sensing of pressure and strain, resistance-based detection of temperature, and ion-signal driven cancer diagnostics emulating the multifunctional sensitivity of natural skin.

Collectively, the intrinsic highwater content of hydrogels is the foundational element empowering them to seamlessly bridge the electronics-biology divide. By minimizing impedance, preserving cellular integrity, and efficiently transducing diverse stimuli, hydrogels establish the basis for stable, multimodal biointerfaces that operate harmoniously within living systems.

2.2.1.2. Modulus matching. Beyond superior hydration, modulus matching is equally pivotal for ensuring the long-term stable function of hydrogel-based biosensors. The elastic modulus of human soft tissues typically spans 10^2 Pa to 10^2 kPa, whereas conventional electronic materials (metals, silicon, and rigid synthetic polymers) fall within the MPa–GPa range (Fig. 2B). This orders-of-magnitude mismatch creates persistent interfacial stress that initiates chronic inflammation, provokes immune responses, and leads to tissue damage post-implantation.

Protein-based hydrogels, among others, naturally bridge this gap by closely mirroring the mechanics of biological tissue. Silk-fibroin hydrogels, for instance, exhibit moduli of 1–150 kPa, aligning closely with the elasticity of skin and internal organs.[52] Gao et al.[53] developed poly (vinyl alcohol) PVA microfiber composite hydrogels (PVA/MF-CH) whose modulus could be precisely tuned to 25–40 kPa via controlled freeze–thaw cycles, all while maintaining over 91.8% water content. This ideal mechanical-hydration combination rendered them highly effective substrates for skin-adhesive sensors, ensuring both patient comfort and stable signal acquisition. Kim et al.[54] introduced tough hydrogel–Ecoflex hybrid substrates whose modulus was comparable to that of skin. Combined with ultrahigh stretchability (strain up to 2000%), these materials maintained stable adhesion and comfort even during dynamic body movements, positioning them as promising candidates for electronic skin and wearable sensing networks. Liu et al.[49] reported conductive hydrogel electrodes with moduli of 24–32 kPa, closely matching peripheral nerve tissues. When implanted into the sciatic nerve of mice, these compliant devices significantly reduced inflammatory responses and preserved axonal integrity compared with rigid cuff electrodes, powerfully highlighting their advantages in implantable applications. Similarly, Spencer et al.[45] developed PEG hydrogel-coated neural implants $E \approx 10$ kPa and compared them against uncoated glass capillaries ($E \approx 70$ kPa) implanted into the rodent brain. Immunofluorescence imaging revealed markedly attenuated GFAP signals surrounding the hydrogel-coated probes, indicating substantially less glial scarring and reduced chronic inflammation (Fig. 2C). This beneficial outcome is directly attributed to the reduction in interfacial strain afforded by the softer implants, which mitigates the mechanical aggravation of glial cells.

2.2.2. Biocompatibility. Biocompatibility ultimately dictates the success and longevity of biosensors in long-term operation. Extensive clinical and engineering studies have consistently revealed that traditional non-hydrogel electrodes suffer from poor tissue compatibility. Deyo et al.[55] reported that approximately one-third of TENS patients experienced skin irritation at electrode sites, with several discontinuing treatment due to severe dermatitis. Likewise, long-term AEEG monitoring showed progressive electrode-site inflammation, with 20–25% of patients suffering moderate to severe reactions.[56] Engineering analyses further indicate that both the adhesive layers and the conductive gel components of Ag/AgCl electrodes can induce skin irritation and contact dermatitis during prolonged use.[57,58]

In sharp contrast, emerging hydrogel-based sensors have consistently demonstrated excellent biocompatibility across diverse material chemistries. Natural polymer-based hydrogels, derived directly from biological sources, inherently exhibit

favorable compatibility. For example, silk fibroin-based hydrogels displayed excellent *in vitro* compatibility: mouse embryonic fibroblasts (MEFs) and human mammary epithelial cells (MCF-10A) cultured in their presence for 24–48 hours exhibited only minor reductions in proliferation, confirming good cellular-level compatibility.[51] Similarly, MeTro hydrogels implanted subcutaneously in rats for 28 days showed seamless integration with host tissue.[50] Histological and immunohistochemical analysis confirmed minimal lymphocyte infiltration, no severe inflammatory reaction, and only a moderate macrophage response, collectively validating favorable *in vivo* biocompatibility.

Synthetic polymer hydrogels, conversely, afford the unique benefit of precise tuning of chemical structures and crosslinking mechanisms, allowing researchers to optimize biocompatibility. Fonseca *et al.*,[47] for instance, developed photocleavable double-network hydrogels that maintained excellent compatibility both before and after degradation. NIH3T cells cultured with intact hydrogels maintained high viability, and cells exposed to degradation products consistently showed survival rates exceeding 80%. Notably, cell viability in the degradation environment was even slightly higher than in the control group after 14 days (Fig. 2E). This unique finding suggests that the degradation process neither releases cytotoxic substances nor impairs cellular function; instead, it may foster a more favorable microenvironment. This demonstrates that such photodegradable hydrogels ensure safety throughout their entire lifecycle, mitigating the risk of chronic inflammation or tissue damage from byproduct accumulation.

To simultaneously achieve mechanical reinforcement, functional expansion, and efficient signal transduction, researchers have also developed composite hydrogels by integrating functional fillers. Maintaining biocompatibility within these composite systems is paramount. For example, PAM-SF/Fe^{3+} hydrogel extracts supported the growth and normal morphology of normal human diploid fibroblasts (NHDF), with CCK-8 assays indicating nearly identical viability to control groups.[59] Similarly, PSAB composite hydrogels sustained high viability of HaCaT keratinocytes over 1, 4, and 7 days of culture, with cells displaying normal morphology comparable to the PVA-B hydrogel control.[60] CNT/gelatin hydrogels, when co-cultured with HEK-293 cells, also demonstrated robust compatibility: significant proliferation was observed after 48 hours, and darkfield microscopy confirmed increased numbers of viable cells, confirming the absence of cytotoxicity[45] (Fig. 2D).

At the tissue level, composite hydrogels frequently outperform conventional flexible substrates. MXene–PAA–ACC hydrogels, for instance, showed nearly 95% cell viability *in vitro* and, critically, caused no allergic reactions in animal skin adhesion tests, confirming compatibility at both the cellular and tissue levels.[63] Similarly, rGO/gelatin hydrogels adhered to human skin without causing adverse effects, whereas PET films, commonly employed as flexible electronic substrates, often induced redness and itching.[48] This contrast emphatically demonstrates the superior skin compatibility of hydrogel-based materials.

Even more importantly, the long-term *in vivo* superiority of hydrogel devices has been confirmed. Liu *et al.*[49] encapsulated elastic microelectronic devices (MECH electrodes), constructed from conductive hydrogels, around the sciatic nerves of freely moving mice for a continuous six-week period, using rigid plastic cuff electrodes (PET/gold films) as controls. Results showed that the fluorescence intensity of neurofilament and S-100 in the MECH group was comparable to that of sham controls, while cuff electrodes showed a marked reduction. Furthermore, inflammatory markers TNF-α and ED1 were slightly lower in the MECH group than in sham controls and were significantly lower than in the rigid cuff electrode groups. Notably, even under conditions of repeated body motion, MECH electrodes caused no nerve damage and induced only mild inflammation, fully demonstrating their outstanding *in vivo* biocompatibility in dynamic tissue environments.

To further substantiate the biocompatibility of hydrogels in functional tissue-repair settings, wound-healing models have been extensively utilized to monitor host responses during the regenerative process. A representative study by Tariq *et al.*[61] involved the development of a polyvinyl alcohol (PVA) hydrogel functionalized with Papaver somniferum extract (PSE), which was evaluated using a full-thickness murine skin wound model. Following a 24 day treatment period, the PSE-PVA hydrogel facilitated approximately 95% wound closure: a significant improvement over both the extract-only treatment (78%) and the untreated control, which lagged at roughly 20%. Beyond macroscopic closure, histological assessments confirmed accelerated re-epithelialization and the formation of well-organized granulation tissue with early-stage regeneration of skin appendages. Notably, the absence of abnormal inflammatory infiltration or tissue necrosis underscores the favorable tissue compatibility of these hydrogel matrices throughout the wound-healing trajectory.

Collectively, insights from both clinical and engineering perspectives underscore a persistent challenge: traditional rigid electrodes entail significant risks of skin irritation, contact dermatitis, and interfacial failure during extended use. Hydrogel-based systems offer a compelling alternative, consistently eliciting favorable biological responses characterized by negligible toxicity, minimal inflammation, and seamless tissue integration. From initial *in vitro* screening to longitudinal *in vivo* implantation, the cumulative evidence identifies superior biocompatibility as the defining advantage of hydrogels over conventional electronic materials. This inherent compatibility establishes the requisite foundation for their translation into the next generation of wearable and implantable clinical diagnostics.

In comparison, elastomeric materials provide exceptional mechanical flexibility and have established a strong track record of biocompatibility across diverse biomedical applications. However, elastomers typically lack the intrinsic hydration and continuous ionic transport pathways necessary for stable bioelectronic coupling. PDMS, for instance, while a staple in biomedical and microfluidic engineering due to its chemical stability, possesses an inherently hydrophobic

surface dictated by its methyl functional groups. This hydrophobicity fundamentally restricts interfacial wettability, complicating the formation of stable, hydrated junctions in aqueous or biological media. While surface modification techniques such as plasma treatment, physiosorption, and chemical grafting have been employed to mitigate this issue, these interventions often suffer from poor long-term stability and introduce undesirable processing complexity.[62]

Hydrogels, by contrast, possess an inherent highwater content that intrinsically mirrors the hydrated microenvironment of native biological tissues. This fundamental hydration not only facilitates seamless ionic transport but also fosters the development of low-impedance, stable biointerfaces without the need for cumbersome surface engineering. Consequently, efficient ion exchange and robust interfacial integrity are maintained even over prolonged durations—attributes that make hydrogels uniquely suited for long-term implantable biosensors operating within the rigors of dynamic physiological environments.

In summary, clinical and engineering data consistently reveal that traditional rigid electrodes pose significant risks of skin irritation, contact dermatitis, and interface failure. In contrast, hydrogel-based systems—whether based on natural, synthetic, or composite polymers, have repeatedly demonstrated non-toxicity, minimal inflammation, and superior tissue integration. Evidence ranging from *in vitro* cell culture studies to long-term *in vivo* implantation confirms that superior biocompatibility is a core, distinguishing advantage of hydrogels over traditional biosensor materials, providing a robust foundation for their application in clinical wearable and implantable devices.

2.2.3. Degradability. Traditional biosensors, typically composed of metals, silicon, and inert polymers, inherently suffer from negligible biodegradability despite their excellent electrical and mechanical performance. This limitation presents two major, cascading challenges. From a clinical perspective, the long-term retention of non-degradable foreign materials

within the body frequently leads to chronic inflammation, debilitating fibrosis, or immune rejection.[69] Due to their persistent nature, such implanted devices routinely necessitate secondary surgical removal, significantly escalating patient risk and burden. Furthermore, the persistent material often induces fibrous capsule formation, which progressively isolates the device from the surrounding tissue, resulting in a significant and deleterious attenuation of signal conduction. Experiments by Turner *et al.*[70] confirmed that even devices exhibiting initial tissue compatibility inevitably trigger sustained immune responses and gliosis upon long-term retention, ultimately leading to functional impairment. From an environmental perspective, the poor degradability of conventional biosensors substantially contributes to the growing issue of electronic waste accumulation, and their disposal *via* landfilling or incineration poses demonstrable ecological and human health risks.[64] In this critical context, hydrogels, with their unique and tunable degradability, offer a crucial pathway to simultaneously address both clinical and environmental imperatives (Table 1).

2.2.3.1. In vivo degradation and clinical safety. Hydrogels demonstrate robust degradability under conditions that mimic the physiological environment. For instance, Di *et al.*[65] developed hydrogels that exhibited significant mass loss and extensive degradation within 50 days in phosphate-buffered saline (PBS) solution. Similarly, Li *et al.*[63] reported that MXene–PAA–ACC hydrogels underwent substantial breakdown within 65 days in PBS solution, strongly supporting their potential for controlled, gradual disintegration in simulated physiological settings. More critically, Zhang *et al.*[52] demonstrated that CSFH-based hydrogels gradually degraded under the enzymatic action of papain, while crucially maintaining reliable sensing performance throughout their service life until complete breakdown. This body of work underscores that degradable hydrogels can not only guarantee stable monitoring during their functional period but also abrogate the clinical risks associated with long-term foreign body retention and the

Table 1 Different types of hydrogels degrade under different conditions

Types of hydrogels	Degradation conditions	Degradation time	Degradation amount	Ref.
Fully physical cross-linked hydrogels	PBS solution at room temperature	50 days	$79.43 \pm 2.3\%$	65
MXene-PAA-ACC hydrogel	PBS solution	65 days	Largely degraded	63
CG hydrogels	PBS solution	13 days	Completely degraded	46
CSFH-based hydrogel	Papain solution with concentration of 0.25%	15 hours	Almost completely degraded	52
AuNP-doped CSFH	532 nm lasers with average radiation power of 100 and 50 mW	1 hour	Completely degraded	52
ONB-1	Irradiation with UV light	1 hour	57%	47
		6 hours	100%	
ONB-2	Irradiation with UV light	1 hour	3%	47
		6 hours	10%	
		24 hours	10%	
3D printable hydrogel	Sodium hydroxide solution (pH = 13)	18.6 minutes	Completely degraded	66
	Sodium hydroxide solution (pH = 14)	58 seconds	Completely degraded	
D_1 hydrogel	Saline solution	114 hours	Completely degraded	67
Ionic PXGN hydrogel	Water	12 hours	Completely degraded	68
Screen-printed RG hydrogel	80 °C hot water	20 seconds	Completely degraded	48
RG hydrogel	Embed into the soil	32 days	Completely degraded	48
TDBS hydrogel	In a 4 cm deep layer of soil	30 days	Completely degraded	71

need for secondary surgical removal once their utility is concluded.

2.2.3.2. Environmental degradation and material sustainability. The degradability of hydrogels is equally vital from a material sustainability perspective. Fonseca *et al.*,[47] for example, designed photocleavable DA hybrid hydrogels that rapidly degraded under UV irradiation *via* the photolysis of *ortho*-nitrobenzyl (ONB) groups, which involved the scission of benzylic C–H bonds at crosslinking sites. Structural modification was shown to critically influence the degradation kinetics: one variant (ONB-1), containing α-CH$_3$ and alkoxy substituents, achieved ~57% bond cleavage within 1 hour of irradiation and completely degraded within 6 hours. Conversely, the unmodified analogue (ONB-2) showed only 10% conversion even after 24 hours, highlighting the power of chemical programmability over degradation rate. Furthermore, 3D printable hydrogels have demonstrated ultrafast degradation under alkaline conditions, dissolving completely within 18.6 minutes at pH = 13 and within just 58 seconds at pH = 14.[66] These findings confirm that external triggers, such as light and alkaline environments, can serve as effective and controllable actuators for rapid hydrogel disintegration.

Even under more moderate, natural conditions, hydrogels display promising degradability. D$_1$ hydrogels, for instance, degraded completely in saline solution within 114 hours.[67] Qu *et al.*[68] reported that ionic PXGN hydrogel dissolved entirely in water within approximately 12 hours. The environmental benefit extends to natural ecosystems, as demonstrated by RG hydrogels buried in soil that achieved full degradation within 32 days.[48] Similarly, TDBS hydrogels completely degraded within 30 days under soil conditions.[71]

2.2.3.3. Recycling and sustainable filler recovery. Notably, some advanced hydrogel systems not only degrade safely but also permit the recovery and reuse of valuable functional fillers, thus directly contributing to a sustainable material cycle. For example, RG6 hydrogels could be cut, reheated, and remolded into specific shapes.[48] The resulting regenerated hydrogels retained mechanical and electrical properties highly comparable to the original samples: tensile strain was reduced by only ~5%, tensile strength maintained at 80%, and both electromagnetic shielding and conductivity saw a minimal reduction of only 5–6% (Fig. 1F, G and H). Similarly, OMDDH hydrogels degraded in hydrochloric acid solution to release embedded MXene fillers, which could then be reassembled into sensors that maintained excellent conductivity.[72] Fu *et al.*[73] further reported that GDIH10-0.06-based sensors could be rapidly dispersed in warm water (45 °C, 800 rpm stirring) within 1 hour, recovered, and successfully regenerated into new sensors. While the regenerated samples exhibited a slight reduction in tensile strength, their ionic conductivity, sensitivity, and strain-sensing performance remained essentially stable, ensuring continued viability for sensing applications.

In conclusion, unlike conventional biosensors that pose persistent clinical and environmental threats, hydrogel systems exhibit controlled and versatile degradability across a variety of physiological, chemical, and environmental conditions. This ability to ensure safe *in vivo* degradation, thereby avoiding secondary surgeries, coupled with the emerging potential for recycling and reuse of functional fillers, establishes degradable hydrogels as a highly promising and ethically responsible material platform for the next generation of sustainable biosensors.

To facilitate comparison of representative hydrogel matrices used in bioelectronic applications, key material parameters reported in recent studies are summarized in Table 2.

3. Sensing mechanism of hydrogel-based wearable and implantable biosensors

Hydrogel-based biosensors convert biochemical or physical stimuli into quantifiable signals by exploiting the intrinsic responsiveness of hydrated polymer networks. The unique advantages of hydrogels allow them to deform, swell, and incorporate functional molecules or nanoparticles, supporting diverse transduction strategies. Broadly, hydrogel sensing mechanisms can be categorized into two principal types: physical and chemical. Each provides distinct advantages and limitations.[13]

Physical transduction relies on the inherent mechanical and ionic responses of the hydrogel network to translate external perturbations into electrical, mechanical, or optical outputs.[74] These mechanisms are valued for their robustness, reversibility, and long-term stability. Chemical transduction, in contrast, integrates molecular recognition events such as binding, catalysis, or cleavage into the hydrogel matrix, generating highly specific and tunable responses to biochemical cues. In practice, most advanced hydrogel sensors operate at the intersection of these two paradigms. By embedding recognition elements within a physically responsive matrix, they allow molecular interactions to alter structural or ionic pathways.[19,75] This coupling unites the selectivity of chemical recognition with the durability of physical transduction, yielding sensors that are both sensitive and resilient (Table 3).

3.1. Physical mechanisms

Physical mechanisms in hydrogel sensors depend on the intrinsic response of the polymer network to external stimuli, including changes in swelling, mechanical deformation, and ionic rearrangement.[76] Fundamentally, a hydrogel is a crosslinked polymer matrix saturated with water and ions. Any disturbance that modifies osmotic balance, mechanical stress, or ionic gradients alters its internal structure, which in turn affects the material's electrical, mechanical, or optical characteristics.

When exposed to fluid or ions, osmotic pressure drives solvent molecules into the polymer network, stretching the chains and expanding the mesh structure. This expansion decreases steric hindrance and facilitates ion mobility, thereby lowering the material's electrical resistance.[77] The degree of

Table 2 Comparison of key performance parameters of representative hydrogel matrices for bioelectronic applications

Hydrogel matrix	Water content	Young's modulus	Biocompatibility outcome	Electrical conductivity	Ref.
PEG-DMA hydrogel	—	11.64 ± 2.0 kPa	Reduced chronic glial scarring *in vivo*	—	45
CNTs/gelatin hydrogel	—	218–983kPa	Supported HEK-293 cell proliferation	0.0015–0.0093 S cm^{-1}	46
Photodegradable DN hybrid hydrogel	—	56.2 ± 3.5 kPa	Non-cytotoxic (>75% viability), supporting fibroblast adhesion and proliferation	—	47
RG hydrogel	—	233.3–2999.2 kPa	Skin-friendly with no skin irritation	0.0018–0.0066 S cm^{-1}	48
Electrically conductive hydrogel	~85 wt%	24 ± 5.4 kPa	Reduced inflammation in sciatic nerve implantation	47.4 ± 1.2 S cm^{-1}	49
MeTro/GO hybrid hydrogel	—	19.3 ± 0.7 kPa	Supported cardiac cell growth, good *in vivo* biocompatibility	Enhanced electrical conductivity with reduced CM excitation threshold	50
Bio-inspired hydrogel	43 wt% (25 °C, 90% RH) 31 wt% (35 °C, skin-mimicking conditions)	~1000 kPa	No cytotoxicity or cutaneous irritation observed	—	51
PVA/MF-CH	$96.3 \pm 0.7\%$ (2 cycles) $92.0 \pm 0.2\%$ (8 cycles)	~25 kPa (4 cycles) ~40 kPa (8 cycles)	Anti-dehydration and skin-friendly	Tunable ionic conductivity *via* salt concentration	53
Hydrogel/ecoflex hybrid substrate	—	~5 kPa	Skin-like low-modulus substrate enabling conformal skin attachment	Stretchable electronic conductivity with stable $\Delta R/R_0$	54
PAM-SF/Fe^{3+} hydrogel	—	10 kPa	Non-cytotoxic	0.2 S cm^{-1}	59
PVA-SA-AgNW-borax hydrogel	—	300–1300 kPa	Non-cytotoxic and antibacterial for skin-contact applications	0.00094 S cm^{-1}	60
MXene-PAA-ACC hydrogel	—	180–300kPa	Non-cytotoxic with high cell viability	Higher conductivity than Ag/AgCl electrodes	63

Table 3 Summary of hydrogel-based biosensors classified by physical and chemical sensing mechanisms

Sensing mechanism	Modality	Active material/hydrogel	Hydrogel functionality	Ref.
Physical	Electrical	Mxene/PVA	Mechanical support	80
	Optical	HPOF/PAM	Chemical functionalization	85
	Electrical	Au nanoparticles/PAM	Antigen uptake	36
	Electrical	ZnO/p(NVCL-coDEGDVE)	Nanostructure/LCST	86
	Electrical	BTO nanocube/PAM	Mechanical support	87
	Ultrasonic	Silica/PAM	Nanostructure	81
	Ultrasonic	Phenylboronic acid/PAM	Nanostructure	82
	Ultrasonic	Mg/p(DMAEMA-DPAEMA)	pH-sensitivity	88
	Ultrasonic	PVA/CMC	Nanostructure	89
Chemical	Electrical	PEDOT:PSS/PAM	Analyte uptake	98
	Optical	Palladium phosphor/gelatin	Adhesion	104
	Optical	Ce6/PDDA	ROS sensitivity	106
	Electrical	PAM/alginate	Mechanical support	102
	Electrical	Collagen-fibrin/genipin	Ionic conduction	103
	Electrical	CBMA	Ionic conduction	110
	Electrical	MgB2/PVA	Nanostructure	113
	Electrical	PEDOT:PSS/PNIPAM/PAM	Impedance matching	114

such swelling arises from the competition between two forces, including the thermodynamic drive for polymer–solvent mixing and the elastic resistance of the polymer network to deformation. While classical polymer physics describes this behavior in terms of equilibrium between osmotic and elastic pressures, real hydrogels often exhibit nonlinear swelling dynamics under large or cyclic deformations due to network heterogeneity and viscoelastic relaxation.[78]

A defining advantage of physical transduction lies in its durability.[79] Because these systems do not depend on fragile biological molecules, they are resistant to enzymatic degradation, denaturation, and leaching. The resulting signals are governed by stable material properties allowing consistent performance across repeated cycles. However, this mechanical stability introduces its own challenges. Over time, baseline drift may occur as hydration equilibria shift, ionic strength

fluctuates, or temperature changes subtly alter polymer mobility. Consequently, careful calibration and environmental buffering are essential to distinguish genuine analyte-induced structural responses from artifacts arising from environmental variations.

3.1.1. Wearable physical sensors. In wearable forms, hydrogels frequently interact directly with body fluids, including sweat, tears, saliva. One foundational approach is swelling-modulated ionic conduction. When a hydrogel absorbs fluid, the polymer chains stretch, pore spaces widen, and ionic mobility increases. These changes manifest as measurable shifts in impedance or resistance between electrodes integrated into or adjacent to the hydrogel. The amplitude of signal change is highly dependent on crosslink density and hydrogel porosity. Networks that are too loosely crosslinked may suffer mechanical collapse or delamination upon repeated swelling cycles, while over-tight networks fail to produce significant signal changes.[83,84]

A complementary physical route is mechanical deformation sensing, often implemented with conductive hydrogels. In these systems, conductive fillers, such as carbon nanotubes (CNTs), graphene flakes, metallic nanowires, are dispersed within a hydrogel matrix to form percolative networks. Mechanical strain changes the geometry of these conductive paths, altering contact resistances and yielding measurable electrical variation. Such composite hydrogels have been applied to track joint motion, respiration, and even micromotions of skin or muscle. A recent example is the MXene–PU/PVA hybrid hydrogel reported by Liu *et al.*,[80] where direct ink writing enabled 3D-printed architectures with tunable gauge factors up to 5.7 and stable sensing across large strain ranges. This functionalization arises from the strong interfacial interactions, hydrogen bonding and physical entanglement, between MXene nanosheets and the PU/PVA double network, which provide both continuous electron pathways and effective stress dissipation, thereby preserving conductivity and structural integrity under repeated deformation (Fig. 3A).

Physical optical transduction constitutes another interesting mechanism. Hydrogels incorporating photonic crystal or inverse opal architectures diffract light based on their internal periodic structure, so swelling or contraction shifts lattice spacing and produces visible color changes. Some sweat patches exploit this principle to visually reflect hydration in real time, so smartphone imaging can convert these shifts into quantitative metrics. Fluorescent dye–loaded hydrogels similarly allow physical changes, *via* swelling or refractive index modulation, to influence fluorescence intensity or lifetime, by altering dye microenvironments, quenching rates, or Förster resonance energy transfer (FRET) paths. A recent demonstration by Guo *et al.*[85] reported a stretchable multimodal photonic sensor based on a hydrogel-coated PDMS optical fiber embedded with upconversion nanoparticles and pH-sensitive dyes. This device simultaneously monitored heartbeat, respiration, skin temperature, and sweat pH in real time, with each stimulus encoded at distinct optical wavelengths to avoid crosstalk. Ultimately, the hydrogel network acted as a responsive transduction layer, where swelling or ion-binding events modulated the local refractive index and emission properties of the immobilized dyes and nanoparticles, while the elastomeric PDMS core ensured efficient optical coupling, enabling stable, multiplexed readouts under continuous deformation.

3.1.2. Implantable physical sensors. For implantable applications, physical mechanisms must operate reliably under mechanical constraints, diffusion limitations, and biological interference. Recent advances demonstrate promising strategies for sustaining long-term functionality under physiological stress.

One established approach is resonance-based swelling sensing. Embedding the hydrogel in an LC resonant circuit, the dielectric constant changes with swelling, shifting the resonance frequency detected wirelessly. This passive approach avoids onboard power, making it attractive for long-term implants. A recent demonstration by Li *et al.*[36] realized a wireless immunoassay using antigen-responsive hydrogels integrated with RF resonators. In the design, antigen molecules grafted into a polymer network are bound by antibody-conjugated AuNPs to form immuno-crosslinks that constrain swelling. Upon exposure to free antigen, these crosslinks are competitively broken, triggering rapid hydrogel expansion. That expansion increases the dielectric constant of the hydrogel dielectric layer in the resonator, shifting its resonance frequency, which can be detected wirelessly. To ensure stable readout, the authors used paired RF resonators and relay coils to suppress artifacts such as misalignment and parasitic capacitance when reading the resonant shift.

Another strategy is piezoelectric–hydrogel hybrids. In these designs, piezoelectric nanoparticles (*e.g.* $BaTiO_3$, ZnO) are embedded in the hydrogel.[86,87] When the surrounding tissue or organ pulses or deforms, mechanical stress translates into an electrical signal *via* the piezoelectric phase. The resulting electromechanical coupling enables the hydrogel to transduce biomechanical motion into localized electrical cues, supporting applications in self-powered biosensors and mechanoresponsive drug delivery.

Physical optical transduction constitutes one sensing route, but an alternative mechanism uses hydrogels' acoustic responsiveness, whose acoustic impedance or scattering properties vary with swelling. Analyte-induced swelling changes acoustic contrast, allowing external ultrasound interrogation of embedded sensors. Although this approach is less mature than electrical resonance techniques, it offers a noninvasive window into implanted hydrogels.

As a proof of concept, Nam *et al.*[81] developed an ultrasonic backscattering hydrogel sensor for pH detection. In their design, a silica-nanoparticle-loaded hydrogel sits on a substrate, creating dual acoustic interfaces (hydrogel/substrate and tissue/substrate) (Fig. 3B). The hydrogel's swelling or deswelling modulates both its thickness and internal attenuation attributing to nanoparticle scattering, thereby altering ultrasonic backscattering. By using differential pulse-echo modes, they resolve the hydrogel response from surrounding tissue, enabling wireless pH readout at ~10 cm distance with ~0.2 pH
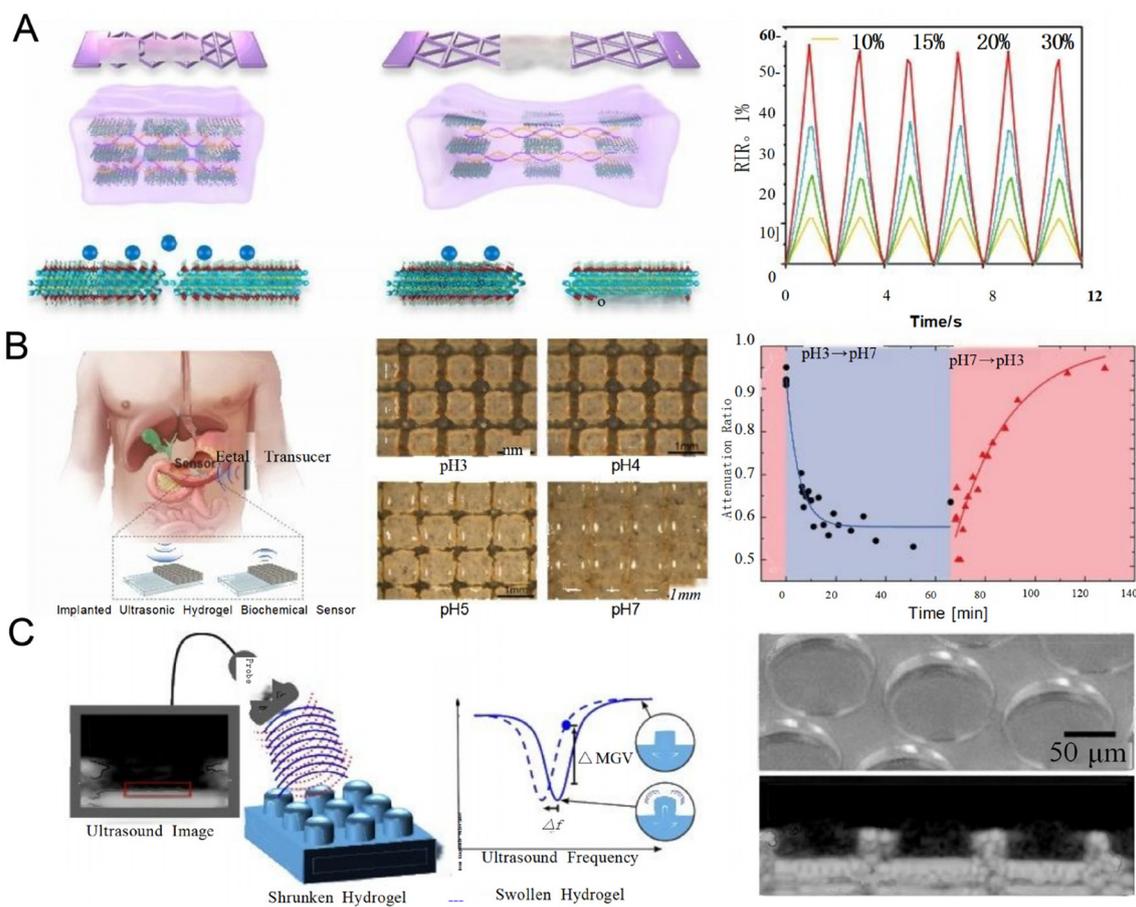
Fig. 3 Hydrogel-based physical sensing mechanisms. (A) Schematic illustration of a strain dependent resistance mechanism, where stretching induces progressive disruption of MXene flake network. Reproduced from Ref. 80 with permission from [Springer Nature], [Haodong Liu *et al.*, *Nature Communications*, 2022] https://doi.org/10.1038/s41467-022-31051-7, under a Creative Commons CC BY 4.0 license, copyright 2022. (B) Volumetric response of patterned silica-loaded hydrogel sensor at different pH levels for remote ultrasound sensing. Reproduced from ref. 81 with permission from [Frontiers Media S.A.], [Juhong Nam *et al.*, *Frontiers in Bioengineering and Biotechnology*, 2020] https://doi.org/10.3389/fbioe.2020.596370, under a Creative Commons CC BY 4.0 license, copyright 2020. (C) Smart hydrogel resonator structure for ultrasound readout. Changes in the resonance frequency of the pillars due to hydrogel swelling results in a change in the intensity of the reflected ultrasound waves. Adapted from Ref. 82 with permission from [American Chemical Society], [Navid Farhoudi *et al.*, *ACS Sensors*, 2020] https://doi.org/10.1021/acssensors.9b02180, copyright 2020.

limit of detection. Mechanistically, swelling increases the path length through an attenuating medium and decreases nanoparticle density (reducing scattering cross section per volume), which shifts echo amplitudes and interference patterns in ultrasound signals, allowing decoding of analyte concentration. A related strategy was demonstrated by Farhoudi *et al.*,[82] who patterned smart hydrogels into micromechanical resonator arrays that coupled volumetric swelling to resonant ultrasound absorption. Their hydrogel pillars exhibited analyte-dependent shifts in resonance frequency, producing grayscale contrast changes in ultrasound images without requiring embedded nanoparticles or electronics, thereby offering a contact-free platform for *in vivo* analyte sensing (Fig. 3C).

In a more recent demonstration, Liu *et al.*[88] introduced bioresorbable, shape-adaptive structures for ultrasonic monitoring of deep-tissue homeostasis. Their system embeds symmetrically distributed bioresorbable metal discs within a pH-

responsive hydrogel. As local chemical changes (*e.g.* pH variation) cause the hydrogel to swell or shrink, the relative spacing between metal discs shifts, altering the acoustic impedance contrast and scattering patterns discernible by ultrasound imaging. This volumetric modulation enables real-time, deep tissue monitoring of physiological status *via* conventional ultrasound.

A major advance in this direction was achieved by Tian *et al.*[89] with the development of an implantable hydrogel-based phononic crystal sensor, or metagel, for continuous and wireless monitoring of internal tissue strains. Their design consists of periodic air columns embedded within a soft, biocompatible PVA/carboxymethyl chitosan double-network hydrogel, forming a two-dimensional phononic crystal whose deformation shifts its ultrasonic bandgap. The bandgapshift manifests as a measurable change in the frequency of ultrasound echoes detected externally through the skin, providing a

wireless readout of strain with sub-percent resolution. The metagel, operating entirely without metal, semiconductor, or chip components, conforms mechanically to soft tissues and maintains stable function for over a month *in vivo* while biodegrading within twelve weeks. By demonstrating long-term, battery-free, and fully biocompatible ultrasound transduction, this system exemplifies how phononic structuring within hydrogels can convert mechanical or biochemical cues into remotely readable acoustic signals, extending hydrogel biosensing into deep-tissue and implantable regimes.

3.2. Chemical mechanisms

Chemical mechanisms in hydrogel sensors incorporate molecular recognition directly into the polymer network, allowing specific binding, catalytic, or cleavage events to trigger local chemical transformations, such as pH shifts, charge redistribution, or crosslink cleavage, that propagate through the material to produce measurable signals. In this framework, the hydrogel acts not as an inert scaffold but as an active transducer, translating molecular recognition into macroscopic response. By integrating selective recognition motifs such as enzymes, aptamers, antibodies, or stimuli-labile linkers, these sensors achieve tunable selectivity toward a broad spectrum of analytes ranging from small metabolites to proteins, nucleic acids, and reactive species.[90,91] The tight coupling between recognition and transduction endows chemical hydrogels with intrinsic amplification capability. A single binding or catalytic event can perturb local equilibrium, propagating structural or ionic changes through the entire matrix and magnifying the output. Design parameters such as the density and spatial distribution of recognition sites, crosslinking degree, and gradient structuring can be tuned to optimize sensitivity and dynamic range. Localization of active motifs near the surface accelerates response time by minimizing diffusion limitations, while embedding them deeper enhances signal stability and averaging over longer timescales.

When a recognition event occurs, the local chemical environment of the hydrogel is altered. A canonical example is the glucose oxidase-based hydrogel sensor, where enzymatic oxidation of glucose generates gluconic acid and hydrogen peroxide. The resulting proton accumulation lowers pH, modulating the ionization state of carboxylate or amine groups within the polymer matrix. These changes shift osmotic pressure and electrostatic interactions, leading to swelling or contraction of the network and concurrent modulation of ionic and dielectric properties. The mechanical and electrical responses thus serve as macroscopic indicators of a microscopic biochemical reaction.[92,93]

Cleavage-based designs follow a similar principle, in which target recognition triggers the rupture of crosslinks within the hydrogel. Reactive oxygen species, specific enzymes, or chemical reductants can cleave labile bonds such as disulfides or boronate esters, converting a dense and rigid structure into a more relaxed, permeable network. This structural transformation manifests as a change in swelling behavior, ion conductivity, or optical transparency, providing a direct transduction pathway from molecular recognition to signal generation.[94]

Selectivity in complex biological fluids poses an additional challenge. Interfering molecules can compete for binding sites or alter the local ionic and pH environment, leading to false signals or drift. Effective implementations often rely on differential sensing schemes, internal reference hydrogels, or ratiometric readouts to isolate the specific response of interest.[95] Achieving long-term stability and reproducibility under such dynamic conditions remains an active frontier in hydrogel biosensor development.[84]

In brief, chemical sensing mechanisms transform hydrogels into intelligent, adaptive materials whose internal chemistry mirrors the complexity of biological recognition. Their programmability and specificity make them powerful platforms for molecular diagnostics and real-time physiological monitoring, though continued advances in stability, antifouling strategies, and multianalyte discrimination are essential for their translation into practical biomedical applications.

3.2.1. Wearable chemical sensors. In hydrogel-based glucose sensing, glucose oxidase (GOx) immobilized within the hydrogel catalyzes glucose oxidation to gluconic acid and hydrogen peroxide (H_2O_2). The generated H_2O_2 is electrochemically oxidized at an electrode, producing current proportional to glucose concentration. The hydrogel functions as a diffusion-limiting barrier, stabilizer, and mechanical buffer. Well-engineered wearable patches achieve detection thresholds around 0.1 mM and linear ranges covering physiological glucose concentrations. Still, the sensor's long-term stability in real biofluids is challenging, since enzyme denaturation, oxidative degradation, or leaching may degrade signal over time. Strategies to mitigate this include enzyme–polymer conjugation, incorporation of protective nanoscaffolds, co-immobilization of catalase to eliminate reactive oxygen species, or encapsulation of the enzyme within nanodomains.[96,97]

Recent advances demonstrate how coupling enzymatic reactions with organic electrochemical transistors (OECTs) can overcome some of these limitations. Bai *et al.*[98] reported a coin-sized, fully integrated continuous glucose monitoring system, where GOx and a redox mediator were covalently immobilized in a hydrogel interfaced with a microneedle array and an OECT amplifier (Fig. 4A). In this design, glucose oxidation triggers a cascade of electron transfers, first to the mediator, then to the transistor gate, where the small electrochemical signal is amplified through the transistor's high transconductance. This architecture not only suppresses noise but also enables tunable sensitivity and stable readout under motion, illustrating how enzymatic sensing can be extended into robust, minimally invasive wearable devices.

In optical chemical sensing, hydrogels loaded with dyes or fluorescent probes enable detection *via* fluorescence or colorimetric variation. Contact-lens hydrogels containing pH- or glucose-responsive fluorophores monitor tear fluid *via* optical signals. Hydrogels embedded with ROS-sensitive dyes respond to oxidative stress, with fluorescence changes indicating metabolic or inflammatory shifts. These systems demand careful control to prevent dye leaching and photobleaching, often addressed by covalent dye tethering or encapsulation within nanoparticle hosts.[99]
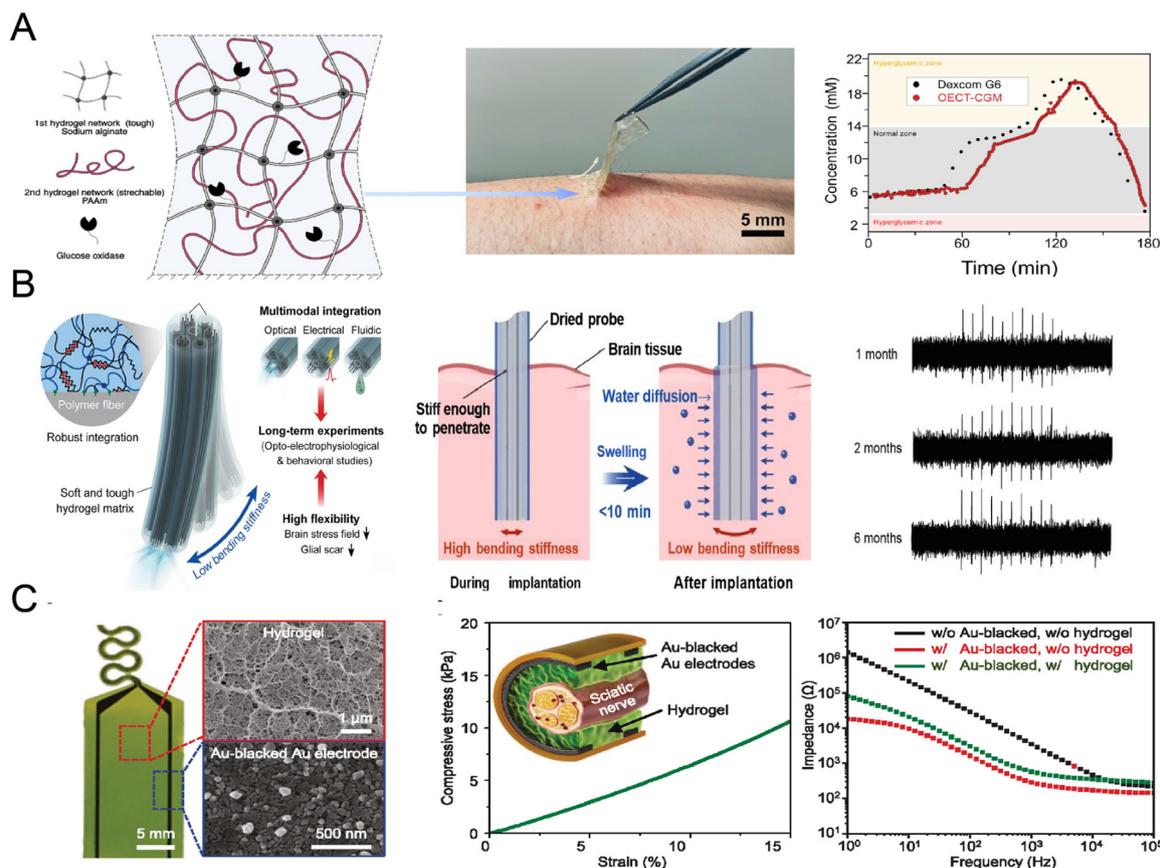
Fig. 4 Hydrogel based chemical sensing and electrophysiological recording. (A) Illustration of the adopted adhesive and soft hydrogel facilitating glucose diffusion for durable real time recording. Reproduced from ref. 98 with permission from [The American Association for the Advancement of Science], [Jing Bai *et al.*, *Science Advances*, 2024] https://doi.org/10.1126/sciadv.adl1856, under a Creative Commons CC BY 4.0 license, copyright 2024. (B) Hydrogel matrix hybridizing multiple individual functional fibers into a multifunctional probe with bending stiffness sufficient for brain insertion. The probe offers stable recording in ventral hippocampus over extended periods. Reproduced from ref. 102 with permission from [Springer Nature], [Seongjun Park *et al.*, *Nature Communications*, 2021] https://doi.org/10.1038/s41467-021-23802-9, under a Creative Commons CC BY 4.0 license, copyright 2021. (C) A genipin-cross-linked gelatin hydrogel with a suitable 3D scaffold was utilized as an intermediate layer between Au-blacked Au electrodes and the sciatic nerve. The mechanical properties (~70.8 kPa) of the hydrogel closely match those of the sciatic nerve. The hydrogel has ion transport properties due to its highwater absorbance, facilitating stable electrical signal transmission. Reproduced from ref. 103 with permission from [Springer Nature], [Kyowon Kang *et al.*, *Nature Communications*, 2024] https://doi.org/10.1038/s41467-023-44064-7, under a Creative Commons CC BY 4.0 license, copyright 2024.

Recent research has further broadened the horizons of hydrogel-based chemical sensing through the development of hybrid architectures tailored for diverse operational environments. A notable example is the work by Pantakitcharoenkul *et al.*,[100] who engineered a hybrid alginate/poly (vinyl alcohol) (PVA) hydrogel for the rapid colorimetric detection of uric acid. By co-immobilizing uricase and horseradish peroxidase within the hydrogel framework, the assay achieved a detection limit of 1.92 μM across a broad linear range (2–600 μM), with a stable readout in under 15 minutes. Crucially, the hydrogel matrix provided a protective microenvironment that significantly enhanced enzyme stability compared to traditional paper-based formats: a testament to the protective efficacy of hydrogel-supported enzymatic platforms. Parallel to advancements in biochemical diagnostics, hydrogel sensors have been increasingly optimized for mechanically demanding or aquatic

settings. For instance, Jiang *et al.*[101] developed an anti-swelling zwitterionic nanocomposite hydrogel, integrating PSBMA with bacterial cellulose nanofibers for underwater applications. The design leverages strong electrostatic interactions within the zwitterionic network to suppress excessive swelling, while the cellulose nanofibers provide the necessary mechanical reinforcement. This synergy resulted in a sensor capable of stable signal transmission and reliable motion detection in aquatic environments, illustrating the versatility of hydrogel platforms across the diverse operational landscapes essential for next-generation wearable and bio-integrated technologies.

3.2.2. Implantable chemical sensors. In implantable settings, chemical hydrogel sensors must operate in a much harsher environment than wearable devices. They must retain specificity amid complex bodily fluids, resist degradation by enzymes and immune processes, and manage diffusion con-

straints while remaining biocompatible. Many of the same design motifs used in wearable chemical sensors carry over, including embedded enzymes, aptamers, or responsive linkers, but with additional burdens in signal drift mitigation, fouling resistance, and long-term stability become paramount.[104,105]

Hydrogels may also be engineered to respond to pathological microenvironments, such as elevated reactive oxygen species (ROS) or acidic pH in tumors and inflamed tissues. In such designs, ROS-sensitive crosslinks like thioketal moieties are cleaved under high oxidative stress, disrupting network connectivity and triggering swelling, structural loosening, or even degradation. As the hydrogel undergoes structural change, embedded reporters or modulated dielectric/optical properties produce a local readout, converting disease-specific chemical cues into measurable signals without the need for external reagents or repeated calibration. Demonstrating this concept, Zhang et al.,[106] developed a hydrogel built around a ROS-responsive conjugated polymer, poly (deca-4,6-diynedioic acid) (PDDA), crosslinked with pullulan. Under high ROS exposure, the PDDA backbone undergoes oxidative cleavage, gradually degrading into biocompatible succinic acid. Concurrently, the hydrogel's intrinsic Raman signal, centered in the cellular "silent window" ($\sim$2121 cm^{-1}), decays in direct correspondence with backbone degradation, thereby enabling in vivo Raman imaging of hydrogel disassembly. In animal models, this material safely co-delivered photosensitizers and immunotherapy agents, while the real-time Raman readout provided a built-in sensing channel of ROS-triggered structural change.

Beyond ROS-responsive frameworks, multimodal implantable hydrogel systems emerge, coupling chemical sensing with optical, electrical, and mechanical readouts. A landmark example is the adaptive multifunctional hydrogel hybrid probe developed by Park and his colleagues.[102] Their architecture integrates a soft hydrogel matrix with embedded optical waveguides, microfluidic channels, and conductive polymer traces (Fig. 4B). The hydrogel serves as a biocompatible, tissue-mimicking substrate that minimizes foreign-body response while mechanically stabilizing the embedded fibers. The implanted hydrogel hybrid probe maintained stable electrophysiological and optogenetic performance for months, demonstrating the feasibility of long-term, multimodal neural interfaces built on mechanically adaptive, tissue-mimetic hydrogels.

Complementing this neural interface concept, Kang et al.[103] introduced a bionic artificial skin that incorporates a fully implantable wireless tactile sensory system based on ionically conductive hydrogel networks (Fig. 4C). Their system integrates soft ionic conductors and pressure-responsive hydrogel layers with stretchable wireless circuits, enabling continuous recording and transmission of tactile signals through biological tissue. The hydrogel encapsulant functions not only as a mechanical cushion but also as an ionic transduction medium that converts mechanical or chemical perturbations into electrical signals while preserving biocompatibility. Long-term implantation studies showed stable operation and minimal

fibrotic encapsulation over several weeks, demonstrating that hydrogel-based ionic conductors can sustain signal fidelity in vivo under repetitive stress.

Together, these studies extend the scope of implantable chemical hydrogel sensors from simple stimulus-responsive chemistries toward integrated, multifunctional architectures capable of optical, electrical, and mechanical transduction. By embedding responsive chemistries within soft, conductive hydrogel matrices and integrating wireless communication modules, next-generation implants can couple biochemical specificity with robust physiological readouts. The continuing convergence of chemical reactivity, ionic conduction, and bioelectronic integration defines a promising pathway toward long-term, intelligent, and fully implantable biosensing systems.

3.3. Strengths, limitations, and strategies for improvement

Hydrogel-based sensing mechanisms offer a versatile and biocompatible platform. Their ability to undergo reversible swelling and mechanical changes enables direct physical transduction, while their chemically functionalizable networks support embedding of recognition elements. These potential sensing mechanisms make hydrogels particularly attractive across the spectrum from epidermal wearables to long-term implants.

However, limitations must be acknowledged. Physical sensors lack molecular discrimination and are sensitive to environmental fluctuations. Chemical sensors face stability challenges from biological degradation or fouling. Implanted devices confront additional complexities of immune response and fibrotic encapsulation, which degrade permeability and mechanical behavior over time.[107,108] Integration into miniaturized, wireless systems while preserving performance is also paramount.[96,97]

To address these limitations, many strategies are in active development. For wearables, zwitterionic polymers are increasingly used to mitigate dehydration. Their balanced cationic and anionic groups form persistent hydration shells through strong ion–dipole interactions with surrounding water molecules, providing intrinsic water retention even under ambient or low-humidity conditions. Recently, Ren et al.,[109] developed a super-tough, non-swelling zwitterionic hydrogel that exploits the Hofmeister effect to stabilize water structure and suppress evaporation under mechanical deformation and thermal stress. In this design, specific ion pairs reorganize the local solvation network around the zwitterionic moieties, strengthening bound water and preventing phase separation or volumetric swelling. The resulting hydrogel maintained mechanical integrity and signal stability after prolonged exposure to air and repeated strain cycles, highlighting how Hofmeister-tuned zwitterionic chemistry can endow hydrogel sensors with long-term hydration stability critical for wearable applications.

Another demonstration is provided by Xu et al.[110] who showed that zwitterionic PCBMA hydrogels can intrinsically generate mobile ions under applied force without added electrolytes, while the zwitterionic segments also provide built-in ion migration channels. Mechanistically, the force-induced dissociation of zwitterionic side groups creates a reversible

supply of charge carriers, ensuring stable conductivity even when environmental hydration levels fluctuate. This mechano-chemical mechanism not only enables high sensitivity up to fivefold greater than nonionic hydrogels, but also avoids reliance on unstable external ions, thereby minimizing drift and supporting stable sensing in diverse environments.

Crosslinking strategies and covalent tethering help stabilize proteins or dyes. A recent example by Zhang *et al.*[111] demonstrates that covalent incorporation of enzymes into hydrogel backbones through site-specific vinyl linkers enables reversible mechanical activation and preserves catalytic integrity over multiple deformation cycles. In their thrombin–hirudin system, genetically engineered enzyme–inhibitor pairs were anchored *via* thiol–ene chemistry, ensuring tight spatial confinement and preventing leaching or denaturation during stress–strain loading. This covalent embedding not only stabilized enzyme activity within the hydrogel matrix but also allowed mechanical cues to modulate catalysis, where structural tethering enhances both stability and functionality of biocatalysts in dynamic hydrogel sensors.

Antifouling coatings (PEG, zwitterion brushes) mitigate protein adsorption in hydrogel implants. Recent advances have shown that microgel-reinforced zwitterionic hydrogels can achieve exceptional nonfouling performance while maintaining mechanical robustness and adhesion. Yao *et al.*[112] developed a poly(carboxybetaine) microgel–reinforced poly(sulfobetaine) (pCBM/pSB) hydrogel coating that forms an interpenetrating entanglement network with the substrate polymer, dramatically enhancing durability and resistance to delamination. The zwitterionic components create a dense hydration layer *via* electrostatic interactions between cationic and anionic groups, preventing nonspecific adsorption of fibrinogen, lysozyme, and platelets even under shear and repeated abrasion. In *ex vivo* circulation tests, pCBM/pSB-coated tubing remained thrombus-free for hours without anticoagulants, illustrating how zwitterionic hydration combined with mechanical reinforcement can yield coatings that simultaneously resist fouling, thrombosis, and inflammation in blood-contacting environments.

Nanocomposite or hybrid hydrogels, incorporating conductive polymers, graphene, or plasmonic particles, boost sensitivity and mechanical resilience. Recent advances have demonstrated that rationally engineered nanocomposite networks can overcome the long-standing trade-off between toughness and conductivity in soft sensing materials. Li *et al.*[113] introduced a bridge crosslinking–dominated hierarchical nanocomposite hydrogel composed of MgB_2 nanosheets and poly(vinyl alcohol), where covalent B–O–C bonds and lamellar alignment produced exceptional strength (8.6–32.7 MPa) and toughness (27.6–123.3 MJ m^{-3}) without sacrificing flexibility. This self-assembly-induced architecture enabled rapid electrical response ($\approx$20 ms) and ultra-low detection thresholds ($\sim$1 Pa) for strain and pressure sensing, outperforming conventional conductive gels. The hierarchical bonding network dissipated mechanical energy through nanosheet pull-out and reversible boronate-ester exchange, providing both resilience

and high sensitivity in deformation-coupled transduction. Such nanocomposite design exemplifies how molecular-scale bridging of inorganic nanosheets with polymer matrices can yield robust, biocompatible hydrogels suitable for next-generation wearable and biomedical sensors.

Self-healing and stretchable double-network hydrogels are being investigated to improve durability under repeated load. Self-healing and stretchable double-network hydrogels are being investigated to improve durability under repeated load. A particularly compelling direction draws from supramolecular and interpenetrating-network design principles exemplified by Jiang *et al.*'s conductive hydrogel interface for wireless wound-monitoring bioelectronics. In that system, a PEDOT:PSS network physically interpenetrated with a thermoresponsive poly(*N*-isopropylacrylamide-*co*-acrylamide) matrix formed a cohesive, low-impedance electrode capable of ~400% reversible strain, stable charge injection over 10 000 cycles, and on-demand adhesion/detachment through thermal transition of the polymer backbone. This architecture illustrates how dynamic crosslinks and dual-network mechanics can decouple deformation from electrical degradation, such strategies mark a convergence between advanced hydrogel mechanics and soft, high-fidelity bioelectronic.[114]

Additionally, transient or biodegradable hydrogels offer a unique solution, by which sensors that dissolve or resorb after a defined period eliminate the need for removal surgery and reduce long-term immunological burden, particularly useful for short-term implants or monitoring phases. Recent developments in fully bioresorbable implant systems demonstrate the potential of such materials for safe, time-limited biomedical operation. For instance, Cho *et al.*[115] designed a fully bioresorbable hybrid opto-electronic neural implant that integrates electrophysiological recording and optogenetic stimulation in a single PLGA-based platform. The device, constructed from biodegradable silicon, molybdenum, and PLGA, conforms to the brain surface and operates reliably for several weeks before completely degrading within two months, leaving no residual materials *in vivo*. This work underscores how transient electronics based on hydrolytically degradable polymers can maintain high biocompatibility and functional integrity while circumventing secondary surgical removal, a principle readily extendable to biodegradable hydrogel-based biosensors for temporary physiological monitoring.

4. Applications of hydrogel-based biosensors

The precise and continuous sensing of biosignals is paramount for advancing fundamental biomedical research, refining clinical diagnostics, and enabling truly personalized therapeutic strategies. Leveraging the multifaceted advantages detailed in the preceding sections (*e.g.*, modulus matching, intrinsic biocompatibility, and stimuli responsiveness), hydrogel-based biosensors have rapidly established a unique and indispensable niche among existing sensing platforms. Consequently, they

have been the subject of extensive investigation across a wide spectrum of biomedical applications. The most significant recent advances in this field can be systematically categorized into two major, interconnected domains: wearable monitoring systems and advanced implantable devices.

4.1. Wearable hydrogel biosensors

A spectrum of human biofluids, including sweat, tears, saliva, and interstitial fluid (ISF), constitutes a rich, readily accessible source of physiological intelligence, harboring abundant biomarkers such as electrolytes, metabolites, hormones, and proteins (Table 4). Given the critical correlation between these analytes and the overall health status, the development of technologies for non-invasive, real-time access and analysis of these biological signals has become a key strategic imperative for advanced health monitoring. Within this dynamic landscape, wearable biosensors have garnered substantial attention due to their inherent flexibility, enhanced comfort, and unparalleled suitability for continuous, integrated monitoring during daily activities. Among the myriad of materials under investigation, hydrogels emerge as exceptionally promising candidates. This is primarily attributed to their aforementioned superior biocompatibility, high water content, and tunable mechanical properties, which facilitate the necessary intimate, stable, and conformal contact with the skin or mucosal surfaces. This section will highlight representative and cutting-edge advances in hydrogel-based wearable biosensors, specifically focusing on their utility in the analysis of sweat, tears, saliva, and ISF.

4.1.1. Interstitial fluid (ISF)-based sensors. Interstitial fluid (ISF), formed *via* plasma filtration across capillary walls, is a highly rich source of physiological information, containing abundant electrolytes, metabolites (*e.g.*, glucose, lactate), hormones, and proteins. It reliably reflects systemic biochemical status, often with only a slight temporal delay relative to blood.

The strong analytical correlation with systemic blood levels renders ISF an invaluable surrogate for invasive blood sampling, particularly in the realm of glucose monitoring. Among the various alternative biofluids currently being explored for non-invasive sensing such as sweat, tears, and saliva, ISF unequivocally represents the most extensively studied and technologically mature system.

Early demonstrations focused on hydrogel microneedle (MN) systems, establishing their feasibility for *in situ* ISF extraction and analyte quantification. Caffarel-Salvador *et al.*[126] reported the first hydrogel-forming MN arrays for both drug and glucose detection *in vivo*. Their poly (methyl vinyl ether-alt-maleic anhydride)/PEG hydrogels were designed to swell upon skin insertion, passively absorbing ISF containing small-molecule drugs and metabolites, with readings correlating well with systemic blood levels. Building upon this foundational concept, Mandal *et al.* engineered polymer-coated MNs that successfully captured[127] both ISF and tissue-resident immune cells, thereby enabling the longitudinal monitoring of local immune responses—a pioneering form of cell-inclusive ISF biosensing.

Hydrogel-based ISF sensors have since rapidly evolved toward fully integrated, multi-analyte, real-time, and long-term platforms. In cutaneous systems, several groups have converged on utilizing conductive and functionally engineered hydrogels that couple the volumetric change of swelling-based ISF uptake with direct on-needle sensing. Odinotski *et al.*[120] developed dopamine-conjugated hyaluronic acid (HA) hydrogels doped with PEDOT:PSS for real-time pH sensing *in vivo*,

Table 4 Comparison of biofluids for health monitoring. Adapted and expanded from ref. 116 with additional data from ref. 117–119

	Molecular weight cutoff	Sample production	Lag time	Na$^+$	K$^+$	Lactate	Glucose	Cortisol	Drug
Plasma	—	—	—	135–145 mM	3.5–5 mM	0.5–10 mM (resting to nonresting)	4.1–6.9 mM (venous, resting)	Hundreds of nanomolar total; tens of nanomolar unbound fraction	Mostly equivalent to unbound in plasma
Sweat	Hundreds of daltons	0.1 to 2 μL min^{-1} cm^{-2}	Ones to tens of minutes	Tens of millimolar	~5–15 mM (under debate)	5–10's mM	~1% of plasma	Unbound similar to plasma	Many equivalent to unbound in plasma
Tear	Hundreds of daltons	~1 μL min^{-1}	~10 min	Hundreds of millimolar	~6–42 mM	1–5 mM	~1% of plasma	Unbound similar to plasma	Many equivalent to unbound in plasma
Saliva	Hundreds of daltons	Tens to hundreds of μL min^{-1} total	Tens of minutes	Tens of millimolar	Tens of millimolar	Tenths to ones of millimolar	~1% of plasma	Unbound similar to plasma	Many equivalent to unbound in plasma
ISF	~1 MDa	Tens of μL min^{-1} cm^{-2}	~5–15 min	Similar to plasma	Similar to plasma	Similar to plasma	Similar to plasma	Unbound similar to plasma	Many equivalent to unbound in plasma

achieving greater than 90% accuracy (Fig. 5A). Zheng *et al.* and Keyvani *et al.*[121,122] further expanded the repertoire of hydrogel-microneedle assays by integrating aptamer probes or electrochemical electrodes for reagent-free detection of glucose, antibiotics, and other critical biomarkers, often combining fluorescence, colorimetric, and voltammetric readouts within a single, unified platform (Fig. 5B and C).

Concurrently, innovations at the material and structural levels have significantly enhanced both conductivity and biorecognition specificity. Ghavami Nejad *et al.*[128] incorporated Ag–Pt nanoparticles and PEDOT:PSS within dopamine–HA hydrogels to achieve enzyme-less electrochemical glucose sensing with high stability. Meanwhile, Dosta *et al.*[129] introduced theranostic MNs that simultaneously delivered immunomodulatory drugs and sampled ISF for immune biomarker profiling in tumors, demonstrating dual diagnostic-therapeutic utility. More recently, the field has progressed to fully inte-

grated skin patches combining swellable MeHA MNs with electrochemical test strips for dual glucose and alcohol analysis,[130] representing a key technological step toward low-cost, user-friendly ISF biosensing. Furthermore, a wearable microneedle platform integrating a protein hydrogel antifouling coating has been reported, enabling long-term and accurate ISF glucose monitoring.[131]

Overall, ISF-based hydrogel biosensors have successfully transitioned from passive fluid sampling tools to sophisticated multifunctional, real-time analytical platforms capable of multiplexed detection and even therapeutic feedback. The seamless integration of conductive polymers, aptamer recognition elements, and miniaturized electronics has firmly established hydrogel MN systems as a cornerstone for next-generation wearable and implantable diagnostics.

4.1.2. Saliva-based sensors. Human saliva, generated by acinar cells within the salivary glands, is a clear, slightly acidic
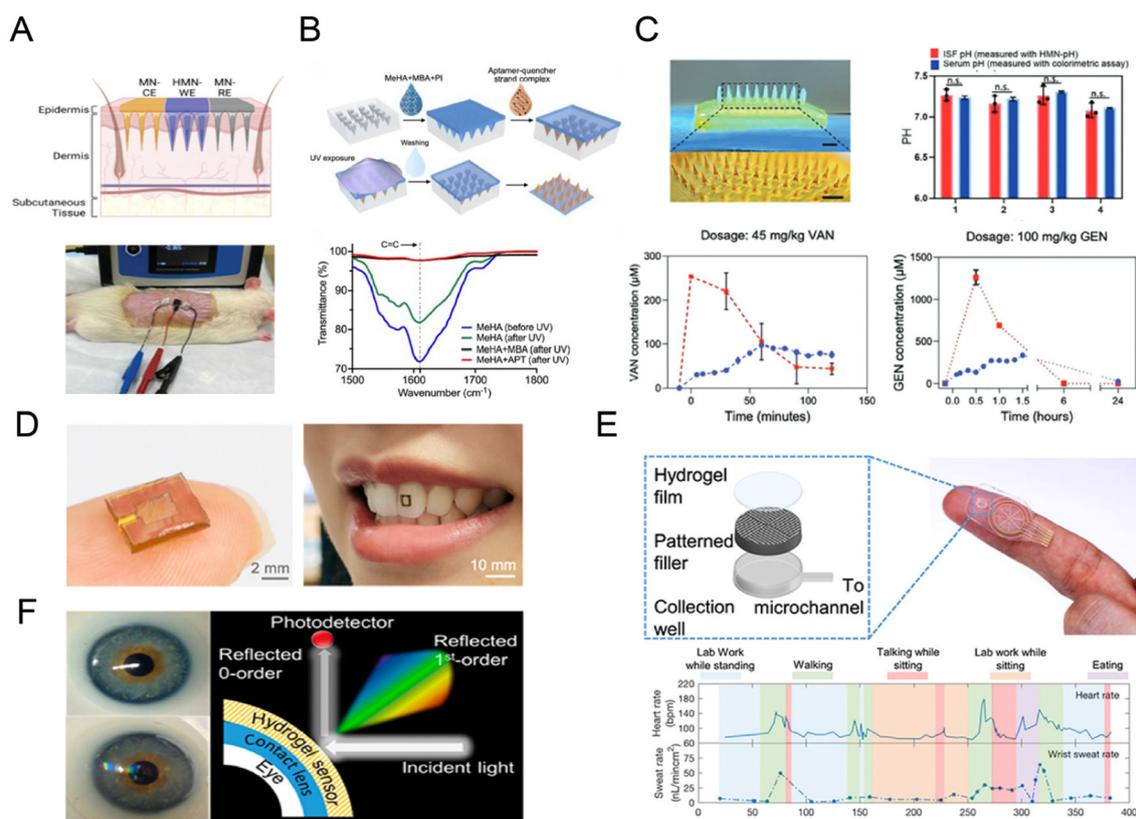

Fig. 5 Representative wearable applications of hydrogel-based biosensors. (A–C) Interstitial fluid (ISF)-based microneedle hydrogel sensors for real-time, minimally invasive drug and biomarker monitoring. A reproduced from ref. 120 with permission from [John Wiley and Sons], [Sarah Odinotski *et al.*, *Small*, 2022] https://doi.org/10.1002/smll.202200201, copyright 2022. B reproduced from ref. 121 with permission from [American Chemical Society], [Hanjia Zheng *et al.*, *ACS Sensors*, 2022] https://doi.org/10.1021/acssensors.2c01033, copyright 2022. C reproduced from ref. 122 with permission from [John Wiley and Sons], [Fatemeh Keyvani *et al.*, *Advanced Science*, 2024] https://doi.org/10.1002/advs.202309027, under a Creative Commons CC BY 4.0 license, copyright 2024. (D) Saliva-based intraoral hydrogel biosensors enabling wireless and real-time detection of multiple analytes. Reproduced from ref. 123 with permission from [Elsevier], [Jingying Pan *et al.*, *Biosensors and Bioelectronics*, 2024] https://doi.org/10.1016/j.bios.2024.116404, copyright 2024. (E) Sweat-based hydrogel microfluidic patch for continuous monitoring of electrolytes and metabolites during daily activities. Reproduced from ref. 124 with permission from [Springer Nature], [Hnin Yin Yin Nyein *et al.*, *Nature Communications*, 2021] https://doi.org/10.1038/s41467-021-22109-z, under a Creative Commons CC BY 4.0 license, copyright 2021. (F) Tear-based hydrogel contact-lens biosensors for optical glucose and multi-biomarker detection. Reproduced from ref. 125 with permission from [American Chemical Society], [Yuqi Shi *et al.*, *Analyst*, 2021] https://doi.org/10.1021/acsnano.8b00829, under a Creative Commons CC BY 3.0 license, copyright 2018.

biofluid composed of water, electrolytes, proteins (e.g., amylase, mucins, IgA), hormones (cortisol, melatonin), metabolites (glucose, lactate, urea), and nucleic acids. This anatomical arrangement where salivary glands exhibit high permeability and are richly enveloped by capillaries facilitates the free molecular exchange between the bloodstream and the neighboring acinar cells.[132] Consequently, saliva contains a rich repertoire of molecular information that is highly capable of communicating an individual's systemic health status. This biochemical richness renders saliva an attractive and distinctive medium for non-invasive monitoring, offering access to hormones and nucleic acids that are often harder to sample in other biofluids. Simultaneously, salivary composition is inherently complex, being strongly influenced by food intake, circadian rhythms, and microbial load, which necessitates rigorous standardization and calibration relative to other biosensing matrices.

Hydrogel-based salivary biosensors are uniquely positioned to address both these opportunities and challenges. By leveraging the high biocompatibility and intrinsic water content of hydrogels, these platforms create soft, hydrated networks that efficiently absorb salivary analytes while simultaneously stably immobilizing enzymes or other specific recognition elements. Recent platforms have integrated these functional hydrogels into wearable mouthguards, intraoral patches, and flexible films, enabling robust electrochemical or optical signal transduction. Crucially, their inherent softness supports comfortable, long-term intraoral wear, while the integration of wireless and smartphone-linked readouts provides the necessary real-time data acquisition for continuous health monitoring.

In recent years, saliva-based hydrogel biosensors have achieved remarkable progress in non-invasive and multi-analyte health monitoring. Tseng et al.[133] developed a tooth-mounted RF-Trilayer sensor incorporating a PNIPAM hydrogel layer to enable wireless pH and temperature sensing directly within the oral cavity. Subsequent studies have focused on improving biochemical specificity and mitigating biofouling: Chen et al.[134] engineered a super-hydrophilic phenylboronic acid hydrogel that achieved sensitive salivary glucose detection while demonstrably reducing bacterial adhesion by over 95%. Liu et al.[135] designed a core–shell PPy/CNT conductive hydrogel, significantly enhancing electron/ion transport and overall electrochemical sensing efficiency.

Furthermore, hydrogel platforms have rapidly expanded their scope to diverse salivary biomarkers. This expansion includes: the development of a Pt nanozyme–hydrogel composite for simple, one-step colorimetric glucose tests.[136] An agarose–AgNP–chlorhexidine hydrogel RF sensor designed for both in situ H_2S monitoring and simultaneous antibacterial therapy[123] (Fig. 5D). A PEDOT/alginate molecularly imprinted hydrogel (MIP) capable of picomolar cortisol detection,[137] showcasing ultra-high selectivity for hormonal monitoring. A hydrogel-based resonant immunosensor enabling the rapid dual detection of CRP and RSV in saliva. de Lima et al.[138] pioneered a tongue-depressor-based multifunctional biosensor that combines hydrogel-assisted electrochemical and colori-

metric modules for accessible self-testing of multiple biomarkers.

Collectively, these pioneering developments underscore a clear and accelerating trend toward the creation of soft, wireless, antifouling, and multifunctional hydrogel systems, a key prerequisite for the future of long-term oral health monitoring and personalized medicine.

4.1.3. Sweat-based sensors. Sweat has garnered significant attention as a non-invasive biofluid for wearable sensing, primarily owing to its ease of collection from the skin surface and its rich composition of electrolytes and metabolites. Sweat glands are distributed across nearly the entire body, providing convenient access for continuous, real-time monitoring of physiological status. Two major types of sweat glands exist: eccrine glands: small, widely distributed, and responsible for thermoregulation by secreting a clear, watery fluid under cholinergic control, and apocrine glands: larger, localized to regions such as the underarm and groin, secreting protein- and lipid-rich fluids in response to emotional or sexual stimuli. Sweat fundamentally consists of water, electrolytes (Na^+, K^+, Cl^-), metabolites (lactate, glucose, urea), and trace proteins and hormones, collectively carrying valuable biochemical information about the body.

Despite these clear advantages, sweat sensing is challenged by several inherent factors. Freshly secreted sweat can be contaminated by skin residues or mixed with previously secreted sweat, while macromolecules such as proteins are often highly diluted due to filtration across glandular membranes.[139] These factors complicate the pursuit of accurate analyte quantification and necessitate advanced strategies for calibration, antifouling, and robust microfluidic flow control.

Hydrogel-based sweat biosensors are uniquely designed to mitigate these critical issues by integrating soft, hydrated networks that promote highly efficient sweat absorption and the stable immobilization of enzymes or other specific recognition elements. Their inherent mechanical compliance ensures conformal, low-noise skin contact and minimizes undesirable evaporative signal drift. When seamlessly combined with epidermal electronics, these hydrogel systems enable continuous, wireless, and real-time monitoring of electrolytes, metabolites, and hormones during dynamic daily activities.

Recent years have witnessed remarkable progress in hydrogel-based sweat biosensors, enabling more reliable and non-invasive access to physiological information. Lin et al.[117] reported thin hydrogel micro-patches capable of passively harvesting natural perspiration without the need for active stimulation, thereby significantly improving the accuracy of lactate and caffeine monitoring while integrating wireless electrochemical readout systems. To address the challenge of low secretion rates during sedentary states, a hydrogel-assisted microfluidic patch was engineered for continuous analysis of thermoregulatory sweat at rest, incorporating pH, chloride, and levodopa sensors for applications ranging from stress evaluation to Parkinson's disease management[124] (Fig. 5E). Tang et al.[140] further demonstrated a touch-based fingertip cortisol sensor utilizing a porous PVA hydrogel for rapid,

stress-free sweat collection coupled with molecularly imprinted polymer electrodes, enabling accurate circadian rhythm and acute stress monitoring. Beyond stress biomarkers, a multifunctional conductive hydrogel sensor was designed for simultaneous pH and tyrosine detection, where the incorporation of CNTs and Ag nanoparticles enhanced conductivity, mechanical robustness, and antibacterial properties.[141] In parallel, Lee et al.[142] pioneered a disposable sweat glucose monitoring patch that integrates hydrogel microneedles for multistage, feedback-controlled transdermal drug delivery, representing a pivotal step toward a closed-loop diabetes management platform.

Together, these cutting-edge advances underscore the versatility and necessity of hydrogel interfaces in sweat sensing, ranging from enhancing sampling efficiency and mechanical stability to enabling sophisticated multimodal, real-time, and even theranostic applications.

4.1.4. Tear-based sensors.
Tear fluid is secreted primarily by the lacrimal glands, with critical additional contributions from accessory glands, meibomian glands, and conjunctival goblet cells, collectively forming the essential trilaminar tear film. Its composition is highly diverse, encompassing water, electrolytes, metabolites, vitamins, amino acids, proteins (such as lysozyme and lactoferrin), cytokines, growth factors, and extracellular vesicles. While some molecules are secreted locally, others are systemically derived from the bloodstream, thereby establishing a vital physiological bridge between ocular and systemic health states.

Among the biofluids investigated for non-invasive health monitoring, tears present one of the most technically debated and challenging media. The available sample volume is typically in the microliter (μL) range, which makes continuous and standardized collection technically demanding and highly susceptible to dilution or evaporation artifacts. Tear composition is further complicated by secretion type (basal *versus* reflex), environmental factors, and significant interindividual variability, often leading to discrepancies in reported analyte levels across studies. While several metabolites and hormones show promising correlations with blood, the stability and clinical utility of these relationships under diverse physiological conditions require rigorous validation. Furthermore, tears contain a considerable proportion of locally secreted proteins and immune factors (*e.g.*, lysozyme and lactoferrin) which, while providing valuable insights into ocular physiology, can complicate their interpretation as systemic biomarkers. Current collection strategies including contact lens-based, flexible eye patch, and eyeglass-based biosensors, each face inherent trade-offs concerning comfort, minimal disturbance of natural tear secretion, and stability. Overall, tears remain a highly promising diagnostic biofluid, but successful clinical translation necessitates addressing persistent challenges in sampling, standardization, and *in vivo* signal correlation.

Over the past decade, tear-based wearable biosensors have rapidly evolved from conceptual prototypes to multifunctional diagnostic platforms, driven by pivotal advances in hydrogel engineering, nanomaterials, and microelectronics. Early efforts, such as the smart contact lens developed by Google and Novartis,[143] established the proof-of-concept for embedding microchips and glucose sensors within soft hydrogel matrices for non-invasive glucose monitoring, simultaneously highlighting both the promise and the technical hurdles of tear–blood glucose correlation and signal stability. Subsequent research has strategically focused on enhancing sensitivity, biocompatibility, and response speed through material innovation: phenylboronic acid–functionalized hydrogels integrated with photonic microstructures enabled optical glucose readout *via* smartphone interfaces[125] (Fig. 5F). Bi-metallic Au–Pt nano-catalysts immobilized in nanoporous hydrogels achieved long-term, hysteresis-free glucose sensing with high accuracy in diabetic animal models.[144]

These developments collectively mark a critical transition toward robust, real-time tear analysis compatible with continuous health monitoring. In parallel, the field is witnessing crucial diversification beyond glucose detection toward multiplexed and microfluidic systems. Clinical trials utilizing the NovioSense eyelid-insert biosensor demonstrated the first reliable correlation between tear and blood glucose in humans,[145] providing powerful validation for the translational potential of tear sensing. Moreover, new form factors, such as wearable eye-patch sensors, now enable simultaneous colorimetric detection of multiple biomarkers (*e.g.*, pH, proteins, ascorbic acid, glucose) within seconds, integrated with smartphone-based analysis.[146]

Collectively, these emerging trends signal a decisive shift toward next-generation ocular biosensing systems that expertly combine soft, adaptive hydrogel materials, multimodal detection capabilities, and seamless wireless data connectivity, paving the way for personalized, continuous, and truly non-invasive health monitoring.

4.2. Implantable hydrogel biosensors

Implantable hydrogel biosensors have emerged as a pivotal class of soft bioelectronic interfaces, specifically engineered for high-fidelity monitoring within the complex milieu of internal tissues. Unlike traditional rigid silicon or metallic sensors, which frequently succumb to mechanical mismatch and chronic fibrosis, hydrogels offer a suite of advantages that transcend even those of established soft elastomers like PDMS or polyimide.[3] As intrinsically hydrated 3D polymer networks, hydrogels possess a characteristic porosity that not only ensures intimate tissue coupling but also facilitates the free diffusion of metabolic fuels, signaling molecules, and ions—transport features largely absent in dense, solid-state soft materials. Furthermore, sophisticated hydrogel formulations can be tailored to mimic the biochemical and structural cues of the native extracellular matrix (ECM), effectively fostering bio-integration while mitigating host inflammatory responses. This biomimetic quality, coupled with an inherent ion-conducting nature, allows for significantly lower interfacial impedance and superior signal transduction compared to non-porous alternatives. Such synergy enables hydrogel-based devices to conform seamlessly to delicate neural or cardiac

architectures, preserving a hydrated microenvironment that maintains the physiological phenotype of adjacent cells. With recent innovations integrating conductive polymers, nanocomposites, and self-healing chemistries, these platforms now support stable electrochemical and optical sensing of diverse analytes, from neurotransmitters to inflammatory markers. Taken together, these attributes solidify the role of implantable hydrogels as a cornerstone for continuous *in vivo* diagnostics and future closed-loop therapeutic architectures.

4.2.1. Subcutaneous implants. Subcutaneous implantation offers a highly accessible and minimally invasive site for continuous biochemical monitoring, a potential most prominently realized by several advanced hydrogel-based glucose sensors. A key innovation involves the integration of a phenylboronic acid (PBA)-functionalized hydrogel interlayer within a passive, wireless radio frequency (RF) resonator.[152] In this system, glucose binding induces volumetric and dielectric changes in the hydrogel, which are precisely translated into distinct shifts in the resonator's frequency. Crucially, this platform requires no on-site electronics or power supply, enabling remote, long-term readout *via* near-field coupling while demonstrating remarkable signal stability without drift over 45 days. Similarly, an ultrasound-resonant implant, composed of glucose-responsive boronic acid hydrogels, achieved real-time *in vivo* glucose monitoring in rat subcutaneous tissue.[153] Here, the swelling- or deswelling-induced resonance changes were detected using a standard external clinical ultrasound probe. By deliberately eliminating complex electronic circuits and leveraging purely mechanical or dielectric transduction mechanisms, these subcutaneous hydrogel sensors effectively overcome the long-standing challenges associated with conventional electronic implants: namely, biocompatibility, on-site power dependence, and wireless communication. These devices thus offer a compelling blueprint for the development of fully biodegradable and retrievable-free implantable devices.

4.2.2. Cardiac implants. The heart, as a continuously beating and highly electroactive organ, imposes stringent and unique requirements on implantable biosensors. Devices intended for cardiac implantation must possess a critical synergy of high electrical conductivity, mechanical compliance, and intrinsic biocompatibility to effectively synchronize with myocardial contraction and ensure stable electromechanical coupling. Furthermore, robust anti-fouling and low-immunogenic properties are essential to prevent fibrotic encapsulation and subsequent signal degradation over the long term. Owing to the complex curvature and continuous mechanical motion of the heart, the sensing interface must also be designed to exhibit exceptional conformality and adhesion, guaranteeing accurate, real-time detection of vital strain, electrophysiological, and biochemical signals.

In recent years, innovative hydrogel-based implantable cardiac biosensors have been developed to meet these formidable demands. Injectable Theranostic Hydrogels: An injectable conductive nanocomposite hydrogel (GNR@SN/Gel), composed of gold nanorods, silicate nanoplatelets, and

PLGA-PEG-PLGA, was fabricated for therapeutic monitoring.[154] This hydrogel was used to encapsulate mesenchymal stem cells and injected into infarcted myocardium, enabling stable electromechanical coupling and *in vivo* PET/CT visualization for real-time assessment of therapeutic efficacy. Enhanced Mechanosensing and Bio-resistance: a wrinkled nanoclay–composite ionic-conductive hydrogel was engineered with a skin-inspired microstructure[147](Fig. 6A). This structural design yielded enhanced stretchability and protein resistance, facilitating the precise *in vivo* localization of myocardial infarction regions. Mechanics-Matched Metamaterials: similarly, a gelatin-based metamaterial hydrogel film (GCF) was constructed, which achieved a precisely tunable modulus (20–420 kPa) and a negative Poisson's ratio to seamlessly match the complex mechanics of soft cardiac tissues.[155] This material was successfully applied for conformal monitoring of cardiac deformation and respiration while concurrently promoting biodegradability and tissue regeneration. LIG-Hydrogel Hybrid Patches: Lu *et al.*[156] demonstrated the creation of a cryogenically transferred laser-induced graphene (LIG)-hydrogel interface using an ultrathin PVA–phytic acid–honey (PPH) hydrogel interlayer. The resulting composite patch was highly stretchable (≈220%) and antibacterial, and was successfully utilized for high-fidelity *in vivo* electrophysiological mapping and arrhythmia diagnosis.

Collectively, these breakthroughs highlight the versatility of hydrogels in serving as the bioelectronic cornerstone for sophisticated cardiac implants, moving beyond simple signal acquisition toward integrated theranostic and regeneration-promoting functionalities.

4.2.3. Neural system implants. Implantable hydrogel biosensors designed for intracranial and neural applications must overcome some of the most stringent engineering and biological constraints among all bioelectronic devices. The brain's ultrasoft and highly dynamic microenvironment, with an elastic modulus typically ranging from only 1–3 kPa, contrasts catastrophically with conventional rigid silicon or metal-based probes (>100 GPa). This profound mechanical mismatch leads to micromotion-induced tissue damage and chronic immune encapsulation (gliosis), which inevitably degrade signal quality over time. Furthermore, the confined intracranial space necessitates miniaturized, highly conformable, and intrinsically biocompatible interfaces that can robustly record or stimulate without generating local inflammation or optical/electrical artifacts, especially when integrating multimodal modalities such as electrophysiology, optogenetics, and ultrasound.

To decisively address these critical challenges, recent advances have leveraged hydrogel materials that mechanically mimic the native softness and ionic conductivity of brain tissue while supporting stable neural interfacing. Topological and Conductive Hydrogels: Shen *et al.*[157] developed topological hydrogels incorporating polyrotaxane cross-linkers and PEDOT:PSS fillers. This design simultaneously achieved a low modulus (~45 kPa), high conductivity, and optical transparency, enabling eight-week stable local field potential (LFP)
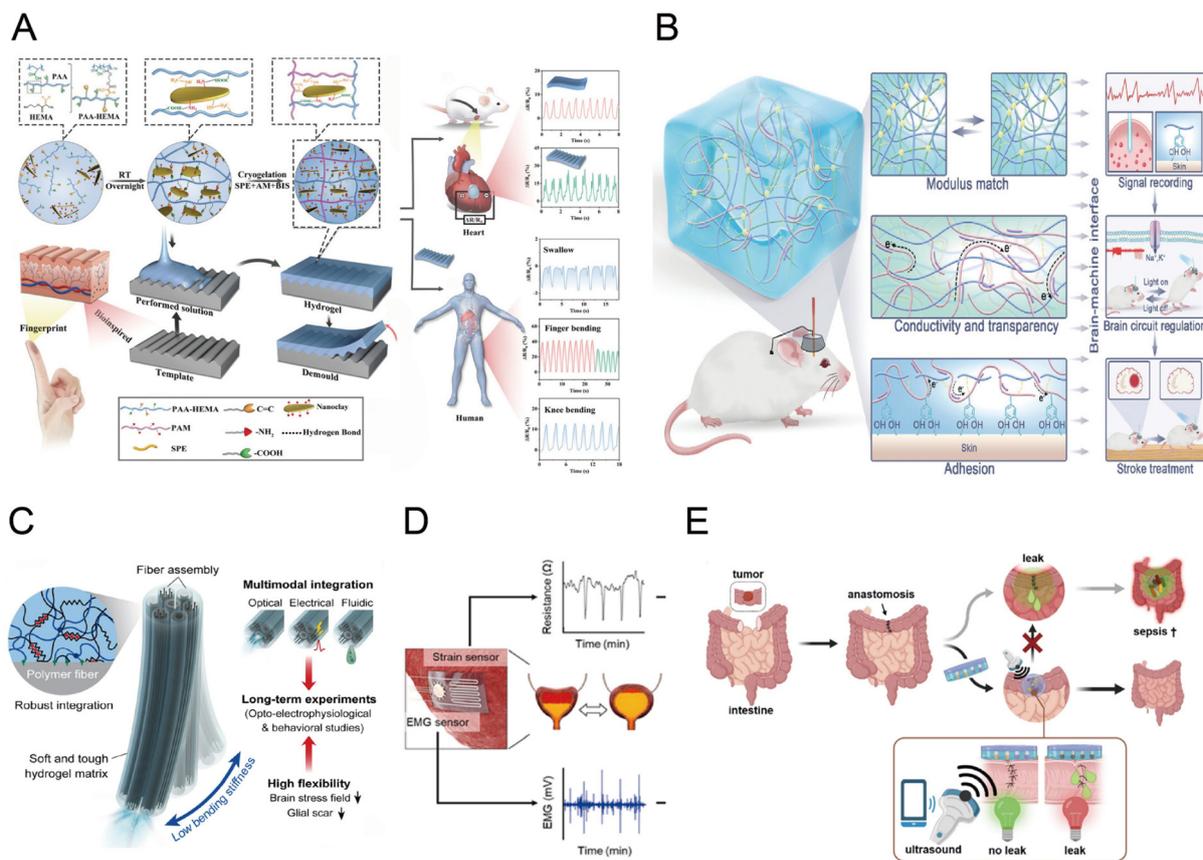
Fig. 6 Representative implantable applications of hydrogel-based biosensors. (A) Wrinkled nanoclay-composite hydrogel for precise detection of myocardial infarction. Reproduced from ref. 147 with permission from [John Wiley and Sons], [Jie Zhang *et al.*, *Advanced Materials*, 2022] https://doi.org/10.1002/adma.202209497, copyright 2023. (B) Amylopectin-based hydrogel probes for brain–machine interfaces. Reproduced from ref. 148 with permission from [John Wiley and Sons], [Yanxia Qin *et al.*, *Advanced Materials*, 2024] https://doi.org/10.1002/adma.202416926, copyright 2024. (C) Adaptive and multifunctional hydrogel hybrid probes for long-term sensing and modulation of neural activity. Reproduced from ref. 149 with permission from [Springer Nature], [Seongjun Park *et al.*, *Nature Communications*, 2021] https://doi.org/10.1038/s41467-021-23802-9, under a Creative Commons CC BY 4.0 license, copyright 2021. (D) Bladder motion and neural activity monitoring. Reproduced from ref. 150 with permission from [Elsevier], [Byungkook Oh *et al.*, *Biosensors and Bioelectronics*, 2023] https://doi.org/10.1016/j.bios.2023.115060, under a Creative Commons CC BY 4.0 license, copyright 2023. (E) Modular stimuli-responsive hydrogel sealants for early gastrointestinal leak detection and containment. Reproduced from ref. 151 with permission from [Springer Nature], [Alexandre H. C. Anthis *et al.*, *Nature Communications*, 2022] https://doi.org/10.1038/s41467-022-34272-y, under a Creative Commons CC BY 4.0 license, copyright 2022.

recording and optogenetic neuromodulation in stroke models. Hydrogen-Bonded Compliant Probes: similarly, Qin *et al.*[148] introduced amylopectin-based double-network (DN) hydrogels (Fig. 6B). The amylopectin promoted the linear rearrangement of PEDOT chains, successfully balancing transparency and conductivity, and formed hydrogen-bonded, compliant brain–probe interfaces with reduced charge transfer resistance and enhanced signal fidelity. These materials facilitated simultaneous neural recording and optogenetic control *in vivo*, demonstrating functional recovery in stroke rats.

Adaptive Multifunctional Hydrogel Hybrid Probes: in another representative strategy, Park *et al.*[149] developed adaptive hydrogel hybrid neural probes by intimately integrating microscale optical, electrical, and fluidic polymer fibers within a soft PAAm–alginate hydrogel matrix that mimics the mechanical softness of brain tissue (Fig. 6C). Owing to the hydration-dependent stiffness transition of the hydrogel, these

probes remained sufficiently stiff for direct insertion in the dehydrated state, but rapidly softened after implantation to reduce micromotion-induced stress and chronic foreign-body responses. This design enabled stable opto-electrophysiological interrogation, drug delivery, and tracking of isolated single-neuron activity for up to 6 months in freely moving mice, highlighting the unique value of hydrogel-based adaptive mechanics for long-term deep-brain interfacing.

Beyond traditional conductive polymers, hybrid and non-electronic hydrogel systems are redefining non-invasive brain sensing. Wireless Ultrasonic Monitoring: Tang *et al.*[158] reported an injectable metastructured "metagel" for wireless ultrasonic monitoring of multiple intracranial parameters—including pressure, temperature, pH, and flow—achieving a deep 10 cm detection depth and full biodegradation within 18 weeks. Shape-Morphing Cortex-Adhesive Sensors: Lee *et al.*[159] designed a shape-morphing cortex-adhesive hydrogel sensor

that combined catechol-alginate adhesives with viscoplastic polymers. This innovation achieved conformal adhesion and artifact-free electrocorticography (ECoG) during closed-loop ultrasound neurostimulation, enabling real-time seizure suppression in rodents.

Together, these pioneering studies illustrate a paradigm shift from rigid electrode architectures toward hydrogel-based, bioadaptive neural interfaces that successfully reconcile conductivity, optical transparency, full biodegradability, and essential mechanical compliance. Such next-generation systems not only permit long-term, high-fidelity monitoring of intracranial biochemical and electrophysiological signals but also uniquely enable multimodal neuromodulation and precise therapeutic intervention within the delicate neural milieu.

4.2.4. Other organ implants. Beyond the established applications in the brain and heart, hydrogel-based implantable biosensors have been successfully extended to a diverse array of internal organs, with each system meticulously engineered to address organ-specific physiological and mechanical constraints.

Bladder Monitoring: an ultra-soft, tissue-adhesive hydrogel sensor was developed specifically for the bladder.[150] This system embedded a liquid-metal strain sensor and Pt-black–coated EMG electrodes within a polyacrylamide matrix. This integration allowed for the simultaneous tracking of detrusor muscle strain and neural activity, effectively resolving the severe modulus mismatch and motion artifacts inherent to continuous bladder monitoring (Fig. 6D).

Gastrointestinal (GI) Tract Diagnostics: in the gastrointestinal tract, ultrasound-responsive hydrogel implants and sealants have emerged as a particularly active direction for postoperative monitoring and complication detection. For example, Anthis et al.[151] developed a modular stimuli-responsive hydrogel sealant patch for early gastrointestinal leak detection and containment, in which pH- and/or enzyme-responsive sensing elements were integrated into an adhesive hydrogel architecture and read out by point-of-care ultrasound imaging. This system enabled early identification of anastomotic leakage while simultaneously providing robust tissue sealing and stable adhesion under harsh digestive conditions (Fig. 6E). More recently, bioresorbable hydrogel–metal composite implants further extended this concept by enabling ultrasound-based monitoring of local pH and homeostatic perturbations in the stomach, intestine, and pancreas 88. These self-resorbing systems represented a minimally invasive strategy for detecting critical postoperative complications while reducing the risks and burdens associated with conventional imaging-based follow-up.

Tendon and Soft Tissue Sensing (Acoustic Metagels): for soft internal tissues like tendons and subcutaneous regions, researchers introduced hydrogel "metagel" sensors.[89] Composed entirely of PVA/CMC hydrogels, these implants leveraged a chip-free phononic design for continuous and wireless strain sensing via ultrasound. This innovation successfully addressed the dual difficulty of achieving biomechanical matching and seamless wireless communication within deep soft tissues.

Vascular Interfaces: at the critical vascular interface, hybrid hydrogel–elastomer microtubes with dynamic wrinkling structures were designed to mechanically mimic arterial compliance and autoregulation.[160] These specialized implants achieved blood-vessel-like hydraulic pressure sensing and flow control through thermally or optically actuated deformation, paving the way for advanced prosthetic vascular systems.

5. Conclusion and perspectives

Hydrogel-based wearable and implantable biosensors have fundamentally redefined the paradigm for interfacing biological and electronic systems, enabling unprecedented opportunities for continuous, high-fidelity health monitoring. By effectively combining high water content, precisely tunable mechanics, and rich chemical functionality, hydrogels successfully bridge the long-standing mechanical and chemical mismatch between rigid, electron-conducting electronics and soft, ion-rich biological tissues. Their intrinsic properties, encompassing ionic–electronic dual conduction, advanced antifouling chemistry, tissue-like compliance, and tailored biodegradability, enable the construction of stable, biocompatible, and multifunctional sensing platforms that operate reliably across diverse and dynamic physiological environments.

Despite the impressive strides in material innovation and device architecture, translating hydrogel-based biosensors from the laboratory to the clinic remains hindered by several formidable technical bottlenecks. Chief among these is long-term operational stability. The very nature of hydrogels, characterized by high water content and dynamic chain mobility, renders them inherently susceptible to dehydration, osmotic swelling–deswelling drift, and progressive structural evolution. In the context of continuous health monitoring, these phenomena often manifest as baseline drift and signal instability, compromising the fidelity of data during chronic wear or implantation. Furthermore, manufacturing scalability and system integration present non-trivial hurdles. The intrinsic softness and aqueous phase of hydrogel matrices are often at odds with standardized high-precision microfabrication techniques, complicating their seamless coupling with conventional rigid electronic backends. Consequently, achieving high-throughput manufacturing that ensures stringent batch-to-batch reproducibility remains an ongoing struggle for the field. Finally, the biointerface itself necessitates further refinement for sustained clinical deployment. While hydrogels are celebrated for their biocompatibility, the dual challenge of maintaining robust interfacial adhesion while simultaneously suppressing long-term inflammatory responses, especially at the delicate tissue-device junction, remains a complex engineering frontier that demands more systematic investigation.

Yet, the robust practical translation of these systems still confronts key engineering and biological challenges. These include preventing dehydration-induced signal drift under

ambient conditions, mitigating biofouling and chronic immune responses *in vivo*, and ensuring signal stability during prolonged operation. A central task remains achieving stable, seamless integration with wireless electronics and miniaturized power modules while concurrently preserving the hydrogel's characteristic softness and biofunctionality. These issues collectively underscore the critical need for rational material design and adaptive device architectures.

Future research efforts must strategically focus on developing zwitterionic or supramolecular chemistries to enhance hydration retention, utilizing nanocomposite reinforcement for superior mechanical resilience, and engineering dynamic crosslinking networks to impart essential self-healing capability and hyper-stretchability. Crucially, the advancement of fully biodegradable and transient systems will further minimize the clinical burden of secondary surgery and mitigate environmental electronic waste.

Transcending traditional physiological sensing, hydrogel platforms are increasingly evolving into multifunctional systems capable of sophisticated wearable and environmental monitoring. A compelling development in this direction includes thermochromic hydrogel photonic devices designed for real-time temperature visualization, where intuitive optical color shifts provide immediate thermal feedback.[161] Beyond temperature, integrated hydrogel systems have demonstrated the capacity for concurrent monitoring of ultraviolet radiation, offering a versatile toolset for personal environmental exposure assessment.[162] The unique combination of intrinsic softness, ionic conductivity, and mechanical adaptability further positions hydrogels as indispensable components in the flexible electronics landscape, facilitating seamless coupling with deformable circuits and energy storage modules.[163] Moreover, the frontier of hydrogel research is shifting toward "all-in-one" biomedical interfaces that consolidate self-healing, antibacterial efficacy, and robust tissue adhesion into a single diagnostic or therapeutic platform.[164] Collectively, these advancements underscore a rapid diversification of the field, signaling a future where research will converge on multifunctional integration, environmental resilience, and the strategic translation of these technologies into clinical practice.

In conclusion, hydrogels have decisively evolved from passive, inert matrices into intelligent, bioadaptive multifunctional interfaces that seamlessly unify sensing, actuation, and biological integration. Through sustained, interdisciplinary collaboration across materials science, bioelectronics, and biomedical engineering, hydrogel-based biosensors are powerfully poised to enable the next generation of durable, adaptive, and truly biointegrated health monitoring technologies.

Author contributions

Y. W. and Y. J. conceptualized the topic of this review. Y. W., Y. G., L. T., Y. G., and B. S. collaboratively wrote the manuscript. Y. W. revised the manuscript. Y. J. supervised the work and provided critical revisions.

Conflicts of interest

There are no conflicts to declare.

Data availability

No primary research results, software or code have been included and no new data were generated or analyzed as part of this review.

Acknowledgements

References

1 I. Uvaliyeva, Z. Idrisheva, D. Borozenets, S. Tezekpayeva, Z. Khassenova and Z. Beldeubayeva, *Eng. Sci.*, 2025, **38**, 1836.

2 A. Paul, A. Srivastava, N. Verma, A. Iqbal, S. K. Maity and H. S. Das, *ES Gen.*, 2025, **9**, 1649.

3 H. Yuk, B. Lu and X. Zhao, *Chem. Soc. Rev.*, 2019, **48**(6), 1642–1667.

4 Y. Liu, M. Pharr and G. A. Salvatore, *ACS Nano*, 2017, **11**(10), 9614–9635.

5 L. Hu, P. L. Chee, S. Sugiarto, Y. Yu, C. Shi and R. Yan, *Adv. Mater.*, 2023, **35**(14), 2205326.

6 A. Joshi, S. Choudhury, A. Majhi, S. Parasuram, V. S. Baghel and S. Chauhan, *Biomater. Sci.*, 2025, **13**(17), 4706–4716.

7 B. Chen, R. Yu, J. Wang, Y. Feng, Y. Zhang and Y. Mao, *Adv. Funct. Mater.*, 2025, e27495.

8 L. Lu, J. Wu, Y. Zhang, C. Liu, Y. Hu and B. Chen, *Nano Res.*, 2025, **18**(11), 94907924.

9 J. Heikenfeld, A. Jajack, J. Rogers, P. Gutruf, L. Tian and T. Pan, *Lab Chip*, 2018, **18**(2), 217–248.

10 W. Gao, S. Emaminejad, H. Y. Y. Nyein, S. Challa, K. Chen and A. Peck, *Nature*, 2016, **529**(7587), 509–514.

11 Z. Lei and P. Wu, *Nat. Commun.*, 2019, **10**(1), 3429.

12 E. M. Ahmed, *J. Adv. Res.*, 2015, **6**, 105–121.

13 A. Herrmann, R. Haag and U. Schedler, *Adv. Healthc. Mater.*, 2021, **10**, 2100062.

14 M. Saeidi, H. Chenani, M. Orouji, M. A. Rastkhiz, N. Bolghanabadi, S. Vakili, Z. Mohamadnia, A. Hatamie and A. Simchi, *Biosensors*, 2023, **13**, 823.

15 K. Völlmecke, R. Afroz, S. Bierbach, L. J. Brenker, S. Frücht, A. Glass, R. Giebelhaus, A. Hoppe, K. Kanemaru and M. Lazarek, *Gels*, 2022, **8**, 768.

16 W. Zhang, Z. Li, Q. Zhang, S. Zheng, Z. Zhang, S. Chen, Z. Wang and D. Zhang, *J. Biomater. Sci., Polym. Ed.*, 2025, **36**, 939–962.

17 G. J. Kim and K. O. Kim, *Sci. Rep.*, 2020, **10**, 18858.

18 N. K. Singh, Y. Wang, C. Wen, B. Davis, X. Wang, K. Lee and Y. Wang, *Nat. Biotechnol.*, 2024, **42**, 1224–1231.

19 P. Zhou, Z. Zhang, F. Mo and Y. Wang, *Adv. Sens. Res.*, 2024, **3**, 2300021.

20 S. Smith, K. Goodge, M. Delaney, A. Struzyk, N. Tansey and M. Frey, *Nanomaterials*, 2020, **10**, 2142.

21 C. D. Spicer, E. T. Pashuck and M. M. Stevens, *Chem. Rev.*, 2018, **118**, 7702–7743.

22 D. Revathi, S. Panda, K. Deshmukh, N. Khotele, V. Murthy and S. K. Pasha, *Polym. Test.*, 2025, **150**, 108912.

23 M. Elsherif, M. U. Hassan, A. K. Yetisen and H. Butt, *ACS Nano*, 2018, **12**, 2283–2291.

24 P. Shen, M. Li, R. Li, B. Han, H. Ma, X. Hou, Y. Zhang and J.-J. Wang, *NPG Asia Mater.*, 2022, **14**, 94.

25 Z. Han, Y. Zhang, Q. Wang, W. Zhang, K. Sui and P. Qi, *Eng. Sci.*, 2025, **36**, 1644.

26 H. Su, L. Mao, X. Chen, P. Liu, J. Pu, Z. Mao, T. Fujiwara, Y. Ma, X. Mao and T. Li, *Adv. Sci.*, 2024, **11**, 2405273.

27 S. Wang, L. Yu, S. Wang, L. Zhang, L. Chen, X. Xu, Z. Song, H. Liu and C. Chen, *Nat. Commun.*, 2022, **13**, 3408.

28 Y. Li, X. Zhang, S. Tan, Z. Li, J. Sun, Y. Li, Z. Xie, Z. Li, F. Han and Y. Liu, *Polymers (Basel)*, 2025, **17**, 1192.

29 S. Agarwala, *Int. J. Bioprint.*, 2020, **6**, 273.

30 Q. Rong, H. Han, F. Feng and Z. Ma, *Sci. Rep.*, 2015, **5**, 11440.

31 H. Xue, D. Wang, M. Jin, H. Gao, X. Wang, L. Xia, D. a. Li, K. Sun, H. Wang and X. Dong, *Microsyst. Nanoeng.*, 2023, **9**, 79.

32 F. Mo, P. Zhou, S. Lin, J. Zhong and Y. Wang, *Adv. Healthcare Mater.*, 2024, **13**, 2401503.

33 X. Wei, H. Wang, Y. Wang, W. Zhang, C. Chen, K. Li, L. Han, J. Rufo, J. Xu and Y. Yao, *Nat. Biomed. Eng.*, 2025, 1–12.

34 S. Mok, S. Al Habyan, C. Ledoux, W. Lee, K. MacDonald, L. McCaffrey and C. Moraes, *Nat. Commun.*, 2020, **11**, 4757.

35 Y. Chen, L. Zhang, X. Wu, X. Sun, N. R. Sundah, C. Y. Wong, A. Natalia, J. K. Tam, D. W.-T. Lim and B. Chowbay, *Nat. Commun.*, 2024, **15**, 8410.

36 X. Li, R. Sun, J. Pan, Z. Shi, Z. An, C. Dai, J. Lv, G. Liu, H. Liang and J. Liu, *Nat. Commun.*, 2024, **15**, 4035.

37 S. Liu, J. Tang, F. Ji, W. Lin and S. Chen, *Gels*, 2022, **8**, 46.

38 M. J. Jensen, A. Peel, R. Horne, J. Chamberlain, L. Xu, M. R. Hansen and C. A. Guymon, *ACS Biomater. Sci. Eng.*, 2021, **7**, 4494–4502.

39 H. L. Bui, H. N. Nguyen, J.-Y. Lai and C.-J. Huang, *Mater. Today Bio*, 2025, 102085.

40 S. Moayedi, W. Xia, L. Lundergan, H. Yuan and J. Xu, *Langmuir*, 2024, **40**, 23125–23145.

41 J. Sabaté del Río, O. Y. Henry, P. Jolly and D. E. Ingber, *Nat. Nanotechnol.*, 2019, **14**, 1143–1149.

42 D. Wang, H. Xue, L. Xia, Z. Li, Y. Zhao, X. Fan, K. Sun, H. Wang, T. Hamalainen and C. Zhang, *Microsyst. Nanoeng.*, 2025, **11**, 105.

43 H.-A. S. Tohamy, *Sci. Rep.*, 2025, **15**, 741.

44 W. Gao, Z. Yan, H. Zhou, Y. Xie, H. Wang, J. Yang, J. Yu, C. Ni, P. Liu and M. Xie, *J. Nanobiotechnol.*, 2025, **23**, 498.

45 K. C. Spencer, J. C. Sy, K. B. Ramadi, A. M. Graybiel, R. Langer and M. J. Cima, *Sci. Rep.*, 2017, **7**, 1952.

46 R. Yin, C. Zhang, J. Shao, Y. Chen, A. Yin, Q. Feng, S. Chen, F. Peng, X. Ma and C.-Y. Xu, *J. Mater. Sci. Technol.*, 2023, **145**, 83–92.

47 R. G. Fonseca, F. D. Bon, P. Pereira, F. M. Carvalho, M. Freitas, M. Tavakoli, A. C. Serra, A. C. Fonseca and J. F. Coelho, *Mater. Today Bio*, 2022, **15**, 100325.

48 R. Yin, C. Zhang, Y. Chen, Y. Wang, Q. Feng, Y. Liu, M. Yu, Y. Yuan, C.-Y. Xu and F. Liu, *Chem. Eng. J.*, 2023, **475**, 145794.

49 Y. Liu, J. Liu, S. Chen, T. Lei, Y. Kim, S. Niu, H. Wang, X. Wang, A. M. Foudeh and J. B.-H. Tok, *Nat. Biomed. Eng.*, 2019, **3**, 58–68.

50 N. Annabi, S. R. Shin, A. Tamayol, M. M. Miscuglio, M. M. Afshar, A. Assmann, P. Mostafalu, J.-Y. Sun, S. Mithieux and M. L. Cheung, *Adv. Mater.*, 2015, **28**, 40.

51 Z. Lei, W. Zhu, X. Zhang, X. Wang and P. Wu, *Adv. Funct. Mater.*, 2021, **31**, 2008020.

52 S. Zhang, Z. Zhou, J. Zhong, Z. Shi, Y. Mao and T. H. Tao, *Adv. Sci.*, 2020, **7**, 1903802.

53 Q. Gao, F. Sun, Y. Li, L. Li, M. Liu, S. Wang, Y. Wang, T. Li, L. Liu and S. Feng, *Nano-Micro Lett.*, 2023, **15**, 139.

54 S. H. Kim, S. Jung, I. S. Yoon, C. Lee, Y. Oh and J. M. Hong, *Adv. Mater.*, 2018, **30**, 1800109.

55 R. A. Deyo, N. E. Walsh, D. C. Martin, L. S. Schoenfeld and S. Ramamurthy, *N. Engl. J. Med.*, 1990, **322**, 1627–1634.

56 S. Ouchida, A. Nikpour, G. Fairbrother and M. Senturias, *Neurodiagn. J.*, 2019, **59**, 219–231.

57 B. Taji, S. Shirmohammadi, V. Groza and I. Batkin, *IEEE Trans. Instrum. Meas.*, 2013, **63**, 1412–1422.

58 H. Wu, G. Yang, K. Zhu, S. Liu, W. Guo, Z. Jiang and Z. Li, *Adv. Sci.*, 2021, **8**, 2001938.

59 J. Li, Q. Ban, M. Xu, S. Wang, J. Geng, Z. Zhang, C. Li, X. Cui, Z. Gu and H. Xu, *J. Colloid Interface Sci.*, 2025, **691**, 137455.

60 L. Fan, L. Hu, J. Xie, Z. He, Y. Zheng, D. Wei, D. Yao and F. Su, *Biomater. Sci.*, 2021, **9**, 5884–5896.

61 F. Tariq, A. Shehzad, M. Ul-Islam, A. Al-Saidi, S. Manan and F. Subhan, *Eng. Sci.*, 2025, **39**, 1958.

62 I. Miranda, A. Souza, P. Sousa, J. Ribeiro, E. M. Castanheira and R. Lima, *J. Funct. Biomater.*, 2021, **13**(1), 2.

63 X. Li, L. He, Y. Li, M. Chao, M. Li, P. Wan and L. Zhang, *ACS Nano*, 2021, **15**, 7765–7773.

64 L. Jia, Y. Li, A. Ren, T. Xiang and S. Zhou, *ACS Appl. Mater. Interfaces*, 2024, **16**, 32887–32905.

65 X. Di, L. Li, Q. Jin, R. Yang, Y. Li, X. Wang, G. Wu and C. Yuan, *Small*, 2024, **20**, 2403955.

66 Y. Zhang, L. Chen, M. Xie, Z. Zhan, D. Yang, P. Cheng, H. Duan, Q. Ge and Z. Wang, *Mater. Today Phys.*, 2022, **27**, 100794.

67 J. Hu, F. Shan, Y. Tian, J. Wei, Z. Chen, W. Liu, G. Chen and G. Fu, *Chem. Eng. J.*, 2025, **504**, 158837.

68 J. Qu, Q. Yuan, Z. Li, Z. Wang, F. Xu, Q. Fan, M. Zhang, X. Qian, X. Wang and X. Wang, *Nano Energy*, 2023, **111**, 108387.

69 J. M. Anderson, A. Rodriguez and D. T. Chang, *Semin. Immunol.*, 2008, **20**, 86–100.

70 J. Turner, W. Shain, D. Szarowski, M. Andersen, S. Martins, M. Isaacson and H. Craighead, *Exp. Neurol.*, 1999, **156**, 33–49.

71 H. Fu, B. Wang, J. Li, D. Cao, W. Zhang, J. Xu, J. Li, J. Zeng, W. Gao and K. Chen, *Mater. Horiz.*, 2024, **11**, 1588–1596.

72 Y. Liu, X. Lv, Y. Song, Q. Ao, B. Yuan, T. Huang, X. Tong and J. Tang, *ACS Sustainable Chem. Eng.*, 2023, **11**, 4177–4186.

73 H. Fu, B. Wang, J. Li, J. Xu, J. Li, J. Zeng, W. Gao and K. Chen, *Mater. Horiz.*, 2022, **9**, 1412–1421.

74 H. Cao, L. Duan, Y. Zhang, J. Cao and K. Zhang, *Signal Transduct. Target. Ther.*, 2021, **6**, 426.

75 C. Zhang, Y. Kang, G. Li, J. Zhou, C. Yao, H. Zeng, C. Wu and J. Wang, *J. Polym. Sci.*, 2025, 4758–4785.

76 L. Tang, S. Wu, J. Qu, L. Gong and J. Tang, *Materials*, 2020, **13**, 3947.

77 H. Tian, C. Wang, Y. Chen, L. Zheng, H. Jing, L. Xu, X. Wang, Y. Liu and J. Hao, *Sci. Adv.*, 2023, **9**, eadd6950.

78 S. Chen, R. Huang and K. Ravi-Chandar, *Int. J. Solids Struct.*, 2020, **195**, 43–56.

79 Z. Fan, D. Ji and J. Kim, *Adv. Intell. Syst.*, 2023, **5**, 2300194.

80 H. Liu, C. Du, L. Liao, H. Zhang, H. Zhou, W. Zhou, T. Ren, Z. Sun, Y. Lu and Z. Nie, *Nat. Commun.*, 2022, **13**, 3420.

81 J. Nam, E. Byun, H. Shim, E. Kim, S. Islam, M. Park, A. Kim and S. H. Song, *Front. Bioeng. Biotechnol.*, 2020, **8**, 596370.

82 N. Farhoudi, H.-Y. Leu, L. B. Laurentius, J. J. Magda, F. Solzbacher and C. F. Reiche, *ACS Sens.*, 2020, **5**, 1882–1889.

83 F. Mo, Y. Lin, Y. Liu, P. Zhou, J. Yang, Z. Ji and Y. Wang, *Mater. Sci. Eng., R*, 2025, **165**, 100989.

84 J. Wu, J. Hong, X. Gao, Y. Wang, W. Wang, H. Zhang, J. Park, W. Shi and W. Guo, *Gels*, 2025, **11**, 589.

85 J. Guo, J. Tuo, J. Sun, Z. Li, X. Guo, Y. Chen, R. Cai, J. Zhong and L. Xu, *Adv. Mater.*, 2025, **37**, 2412322.

86 T. AbuAli, P. Schäffner, M. Belegratis, G. Schider, B. Stadlober and A. M. Coclite, *Adv. Mater. Technol.*, 2022, **7**, 2200246.

87 Z. Wang, Z. Liu, G. Zhao, Z. Zhang, X. Zhao, X. Wan, Y. Zhang, Z. L. Wang and L. Li, *ACS Nano*, 2022, **16**, 1661–1670.

88 J. Liu, N. Liu, Y. Xu, M. Wu, H. Zhang, Y. Wang, Y. Yan, A. Hill, R. Song and Z. Xu, *Science*, 2024, **383**, 1096–1103.

89 Y. Tian, Y. Yang, H. Tang, J. Wang, N. Li, Y. Cheng, T. Kang, J. Tang, M. Zhou and W. Chen, *Nat. Biomed. Eng.*, 2025, **9**, 1335–1348.

90 S. Park, A. Gerber, C. Santa, G. Aktug, B. Hengerer, H. A. Clark, U. Jonas, J. Dostalek and K. Sergelen, *J. Am. Chem. Soc.*, 2025, **147**, 11485–11500.

91 L. Abune, B. Davis and Y. Wang, *Wiley Interdisc. Rev.: Nanomed. Nanobiotechnol.*, 2021, **13**, e1731.

92 H. Laurent, D. J. Brockwell and L. Dougan, *Biomacromolecules*, 2025, **26**, 1195–1206.

93 L. M. Johnson, B. D. Fairbanks, K. S. Anseth and C. N. Bowman, *Biomacromolecules*, 2009, **10**, 3114–3121.

94 M. Regato-Herbella, I. Morhenn, D. Mantione, G. Pascuzzi, A. Gallastegui, A. B. C. S. Valle, S. E. Moya, M. Criado-Gonzalez and D. Mecerreyes, *Chem. Mater.*, 2023, **36**, 1262–1272.

95 A. M. L. Piloto, D. S. Ribeiro, J. o. L. Santos and G. Sales, *ACS Appl. Opt. Mater.*, 2023, **2**, 57–67.

96 J. Zhang, J. C. White, G. V. Lowry, J. He, X. Yu, C. Yan, L. Dong, S. Tao and X. Wang, *Nat. Commun.*, 2025, **16**, 3050.

97 Y. Chen, K. X. Fu, R. Cotton, Z. Ou, J. W. Kwak, J.-C. Chien, V. Kesler, H. Y. Y. Nyein, M. Eisenstein and H. T. Soh, *Nat. Biomed. Eng.*, 2025, 1–14.

98 J. Bai, D. Liu, X. Tian, Y. Wang, B. Cui, Y. Yang, S. Dai, W. Lin, J. Zhu and J. Wang, *Sci. Adv.*, 2024, **10**, eadl1856.

99 X. Xia, Y. Hu, N. Jiang and A. K. Yetisen, *ACS Sens.*, 2025, 7231–7251.

100 J. Pantakitcharoenkul, K. Mekkhayai, K. Paengkhumpung, A. Asgharpour, M. Coblyn and W. Pornputtapitak, *Eng. Sci.*, 2025, **34**, 1398.

101 Z. Jiang, R. Sha, Y. He, M. Wang, W. Ma and S. Gao, *Eng. Sci.*, 2024, **31**, 1200.

102 S. Park, H. Yuk, R. Zhao, Y. S. Yim, E. W. Woldeghebriel, J. Kang, A. Canales, Y. Fink, G. B. Choi and X. Zhao, *Nat. Commun.*, 2021, **12**, 3435.

103 K. Kang, S. Ye, C. Jeong, J. Jeong, Y.-s. Ye, J.-Y. Jeong, Y.-J. Kim, S. Lim, T. H. Kim and K. Y. Kim, *Nat. Commun.*, 2024, **15**, 10.

104 D. Chimene, W. Saleem, N. Longbottom, B. Ko, A. S. Jeevarathinam, S. Horn and M. J. McShane, *ACS Appl. Bio Mater.*, 2024, **7**, 3964–3980.

105 D. Yogev, T. Goldberg, A. Arami, S. Tejman-Yarden, T. E. Winkler and B. M. Maoz, *APL Bioeng.*, 2023, **7**, 031506.

106 Y. Zhang, S. Tian, L. Huang, Y. Li, Y. Lu, H. Li, G. Chen, F. Meng, G. L. Liu and X. Yang, *Nat. Commun.*, 2022, **13**, 4553.

107 J. Wu, J. Deng, G. Theocharidis, T. L. Sarrafian, L. G. Griffiths, R. T. Bronson, A. Veves, J. Chen, H. Yuk and X. Zhao, *Nature*, 2024, **630**, 360–367.

108 S. Capuani, G. Malgir, C. Y. X. Chua and A. Grattoni, *Bioeng. Transl. Med.*, 2022, **7**, e10300.

109 J. Ren, G. Chen, H. Yang, J. Zheng, S. Li, C. Zhu, H. Yang and J. Fu, *Adv. Mater.*, 2024, **36**, 2412162.

110 S. Xu, J.-X. Yu, H. Guo, S. Tian, Y. Long, J. Yang and L. Zhang, *Nat. Commun.*, 2023, **14**, 219.

111 K. Zhang, Y. Zhou, J. Zhang, Q. Liu, C. Hanenberg, A. Mourran, X. Wang, X. Gao, Y. Cao, A. Herrmann and L. Zheng, *Nat. Commun.*, 2024, **15**, 249.

112 M. Yao, Z. Wei, J. Li, Z. Guo, Z. Yan, X. Sun, Q. Yu, X. Wu, C. Yu, F. Yao, S. Feng, H. Zhang and J. Li, *Nat. Commun.*, 2022, **13**, 5339.

113 T. Li, H. Qi, Y. Zhao, P. Kumar, C. Zhao, Z. Li, X. Dong, X. Guo, M. Zhao, X. Li, X. Wang, R. Ritchie and W. Zhai, *Sci. Adv.*, 2024, **10**(5), eadk6643.

114 Y. Jiang, A. A. Trotsyuk, S. Niu, D. Henn, K. Chen, C.-C. Shih, M. R. Larson, A. M. Mermin-Bunnell, S. Mittal, J.-C. Lai, A. Saberi, E. Beard, S. Jing, D. Zhong, S. R. Steele, K. Sun, T. Jain, E. Zhao, C. R. Neimeth, W. G. Viana, J. Tang, D. Sivaraj, J. Padmanabhan, M. Rodrigues, D. P. Perrault, A. Chattopadhyay, Z. N. Maan, M. C. Leeolou, C. A. Bonham, S. H. Kwon, H. C. Kussie, K. S. Fischer, G. Gurusankar, K. Liang, K. Zhang, R. Nag, M. P. Snyder, M. Januszyk, G. C. Gurtner and Z. Bao, *Nat. Biotechnol.*, 2023, **41**, 652–662.

115 M. Cho, J.-K. Han, J. Suh, J. J. Kim, J. R. Ryu, I. S. Min, M. Sang, S. Lim, T. S. Kim, K. Kim, K. Kang, K. Hwang, K. Kim, E.-B. Hong, M.-H. Nam, J. Kim, Y. M. Song, G. J. Lee, I.-J. Cho and K. J. Yu, *Nat. Commun.*, 2024, **15**, 2000.

116 J. Heikenfeld, A. Jajack, B. Feldman, S. W. Granger, S. Gaitonde, G. Begtrup and B. A. Katchman, *Nat. Biotechnol.*, 2019, **37**, 407–419.

117 S. Lin, B. Wang, Y. Zhao, R. Shih, X. Cheng, W. Yu, H. Hojaiji, H. Lin, C. Hoffman and D. Ly, *ACS Sens.*, 2019, **5**, 93–102.

118 E. H. Kim, E.-S. Lee, D. Y. Lee and Y.-P. Kim, *Sensors*, 2017, **17**, 2840.

119 S. Dokwal, A. Arya, A. Sachdeva, M. Rathi, S. Sachdeva, P. Prashant, V. Arora and J. Bhutani, *J. Clin. Diagn. Res.*, 2022, **16**, BC08–BC11.

120 S. Odinotski, K. Dhingra, A. GhavamiNejad, H. Zheng, P. GhavamiNejad, H. Gaouda, D. Mohammadrezaei and M. Poudineh, *Small*, 2022, **18**, 2200201.

121 H. Zheng, A. GhavamiNejad, P. GhavamiNejad, M. Samarikhalaj, A. Giacca and M. Poudineh, *ACS Sens.*, 2022, **7**, 2387–2399.

122 F. Keyvani, P. GhavamiNejad, M. A. Saleh, M. Soltani, Y. Zhao, S. Sadeghzadeh, A. Shakeri, P. Chelle, H. Zheng and F. A. Rahman, *Adv. Sci.*, 2024, **11**, 2309027.

123 J. Pan, X. Li, R. Sun, Y. Xu, Z. Shi, C. Dai, H. Wen, R. P. Han, Q. Ye and F. Zhang, *Biosens. Bioelectron.*, 2024, **259**, 116404.

124 H. Y. Y. Nyein, M. Bariya, B. Tran, C. H. Ahn, B. J. Brown, W. Ji, N. Davis and A. Javey, *Nat. Commun.*, 2021, **12**, 1823.

125 M. Elsherif, M. U. Hassan, A. K. Yetisen and H. Butt, *ACS Nano*, 2018, **12**, 5452–5462.

126 E. Caffarel-Salvador, A. J. Brady, E. Eltayib, T. Meng, A. Alonso-Vicente, P. Gonzalez-Vazquez, B. M. Torrisi, E. M. Vicente-Perez, K. Mooney and D. S. Jones, *PLoS One*, 2015, **10**, e0145644.

127 A. Mandal, A. V. Boopathy, L. K. Lam, K. D. Moynihan, M. E. Welch, N. R. Bennett, M. E. Turvey, N. Thai, J. H. Van and J. C. Love, *Sci. Transl. Med.*, 2018, **10**, eaar2227.

128 P. GhavamiNejad, A. GhavamiNejad, H. Zheng, K. Dhingra, M. Samarikhalaj and M. Poudineh, *Adv. Healthcare Mater.*, 2023, **12**, 2202362.

129 P. Dosta, N. Puigmal, A. M. Cryer, A. L. Rodríguez, E. Scott, R. Weissleder, M. A. Miller and N. Artzi, *Theranostics*, 2023, **13**, 1.

130 M. Zheng, Y. Zhang, T. Hu and C. Xu, *Bioeng. Transl. Med.*, 2023, **8**, e10413.

131 X. Tong, T. Jiang, J. Yang, Y. Song, Q. Ao, J. Tang and L. Zhang, *Biosens. Bioelectron.*, 2025, **277**, 117307.

132 J. M. Yoshizawa, C. A. Schafer, J. J. Schafer, J. J. Farrell, B. J. Paster and D. T. Wong, *Clin. Microbiol. Rev.*, 2013, **26**, 781–791.

133 P. Tseng, B. Napier, L. Garbarini, D. L. Kaplan and F. G. Omenetto, *Adv. Mater.*, 2018, **30**, 1703257.

134 T. Chen, J. Pang, X. Liu, N. Chen, C. Wu, Y. Duan, X. You, Q. Dou, C. Yuan and Y. Wang, *Nano Today*, 2024, **55**, 102141.

135 C.-H. Liu, C.-J. Liao, S. Gupta, D.-W. Huang, C.-Y. Lee, Y.-T. Lai and N.-H. Tai, *ACS Appl. Mater. Interfaces*, 2025, **17**, 15836–15848.

136 J. S. Park and J. S. Choi, *Sens. Actuators, B*, 2022, **359**, 131585.

137 J. Wang, L. Sun, Y. Zuo and N. Hui, *Sens. Actuators, B*, 2025, **426**, 137133.

138 L. F. de Lima, A. L. Ferreira, G. H. M. do Nascimento, L. P. Cardoso, M. B. de Jesus and W. R. de Araujo, *Chem. Eng. J.*, 2024, **494**, 152885.

139 J. Heikenfeld, *Electroanalysis*, 2016, **28**, 1242–1249.

140 W. Tang, L. Yin, J. R. Sempionatto, J. M. Moon, H. Teymourian and J. Wang, *Adv. Mater.*, 2021, **33**, 2008465.

141 Z. Xu, X. Qiao, R. Tao, Y. Li, S. Zhao, Y. Cai and X. Luo, *Biosens. Bioelectron.*, 2023, **234**, 115360.

142 H. Lee, C. Song, Y. S. Hong, M. Kim, H. R. Cho, T. Kang, K. Shin, S. H. Choi, T. Hyeon and D.-H. Kim, *Sci. Adv.*, 2017, **3**, e1601314.

143 M. Senior, *Nat. Biotechnol.*, 2014, **32**, 856–857.

144 S. K. Kim, G. H. Lee, C. Jeon, H. H. Han, S. J. Kim, J. W. Mok, C. K. Joo, S. Shin, J. Y. Sim and D. Myung, *Adv. Mater.*, 2022, **34**, 2110536.

145 A. E. Kownacka, D. Vegelyte, M. Joosse, N. Anton, B. J. Toebes, J. Lauko, I. Buzzacchera, K. Lipinska, D. A. Wilson and N. Geelhoed-Duijvestijn, *Biomacromolecules*, 2018, **19**, 4504–4511.

146 J. Xu, X. Tao, X. Liu and L. Yang, *Anal. Chem.*, 2022, **94**, 8659–8667.

147 J. Zhang, S. Shen, R. Lin, J. Huang, C. Pu, P. Chen, Q. Duan, X. You, C. Xu and B. Yan, *Adv. Mater.*, 2023, **35**, 2209497.

148 Y. Qin, H. Zhao, Q. Chang, Y. Liu, Z. Jing, D. Yu, S. M. Mugo, H. Wang and Q. Zhang, *Adv. Mater.*, 2025, **37**, 2416926.

149 S. Park, H. Yuk, R. Zhao, Y. S. Yim, E. W. Woldeghebriel, J. Kang, A. Canales, Y. Fink, G. B. Choi, X. Zhao and P. Anikeeva, *Nat. Commun.*, 2021, **12**(1), 3435.

150 B. Oh, Y.-S. Lim, K. W. Ko, H. Seo, D. J. Kim, D. Kong, J. M. You, H. Kim, T.-S. Kim and S. Park, *Biosens. Bioelectron.*, 2023, **225**, 115060.

151 A. H. Anthis, M. P. Abundo, A. L. Neuer, E. Tsolaki, J. Rosendorf, T. Rduch, F. H. L. Starsich, B. Weisse, V. Liska, A. A. Schlegel, M. G. Shapiro and I. K. Herrman, *Nat. Commun.*, 2022, **13**(1), 7311.

152 M. Dautta, M. Alshetaiwi, J. Escobar and P. Tseng, *Biosens. Bioelectron.*, 2020, **151**, 112004.

153 N. Farhoudi, L. B. Laurentius, J. J. Magda, C. F. Reiche and F. Solzbacher, *ACS Sens.*, 2021, **6**, 3587–3595.

154 K. Zhu, D. Jiang, K. Wang, D. Zheng, Z. Zhu, F. Shao, R. Qian, X. Lan and C. Qin, *J. Nanobiotechnol.*, 2022, **20**, 211.

155 Y. Chen, Y. Zhou, Z. Hu, W. Lu, Z. Li, N. Gao, N. Liu, Y. Li, J. He and Q. Gao, *Nano-Micro Lett.*, 2024, **16**, 34.

156 Y. Lu, G. Yang, S. Wang, Y. Zhang, Y. Jian, L. He, T. Yu, H. Luo, D. Kong and Y. Xianyu, *Nat. Electron.*, 2024, **7**, 51–65.

157 Z. Shen, Q. Liang, Q. Chang, Y. Liu and Q. Zhang, *Adv. Mater.*, 2024, **36**, 2310365.

158 H. Tang, Y. Yang, Z. Liu, W. Li, Y. Zhang, Y. Huang, T. Kang, Y. Yu, N. Li and Y. Tian, *Nature*, 2024, **630**, 84–90.

159 S. Lee, J. Kum, S. Kim, H. Jung, S. An, S. J. Choi, J. H. Choi, J. Kim, K. J. Yu and W. Lee, *Nat. Electron.*, 2024, **7**, 800–814.

160 X. Wen, S. Sun and P. Wu, *Mater. Horiz.*, 2020, **7**, 2150–2157.

161 S. Hariharan, M. Elnemr, S. El Turk and H. Butt, *ES Mater. Manuf.*, 2025, **28**, 1465.

162 M. Elnemr, Y. Halawani, R. A. Elkaffas, R. Elkaffas, Y. A. Samad and M. Hisham, *ES Mater. Manuf.*, 2025, **27**, 1428.

163 Z. Ye, Y. Yu, H. Miao, Y. Liu, X. Huang and C. Zheng, *Eng. Sci.*, 2025, **37**, 1714.

164 L. Tang, D. Shi, Y. Shen, H. Qi, Z. Liu and L. Yang, *ES Mater. Manuf.*, 2025, **28**, 1522.